

Separational Purification of Nitrate from Inedible Biomass Leachate by

Electrodialysis: Fouling Effect

By

María Teresa Acevedo Morantes

Thesis submitted in partial fulfillment of the requirements for the degree of

MASTER OF SCIENCE

In

Chemical Engineering

UNIVERSITY OF PUERTO RICO

MAYAGUEZ CAMPUS

2004

Approved by

Lorenzo Saliceti Piazza, Ph. D.
Member, Graduate Committee

Date

Félix Román, Ph. D.
Member, Graduate Committee

Date

Guillermo Colón, Ph. D.
President, Graduate Committee

Date

Ingrid Padilla, Ph. D.
Graduate School Representative

Date

Nelson Cardona, Ph. D.
Department Chairman

Date

ABSTRACT

The removal of nitrate and potassium from wheat leachate solution was studied using an electrolytic cell in batch recirculation mode for use in advance life support systems (ALSS). The ALSS or CELSS (Controlled Ecological Life Support System) are systems developed to provide all the required basic human needs for long-term space missions. High nitrate and potassium removals were obtained at 5, 6, 7, 8 and 9 volts. Anions removals over 90% were obtained after 200 minutes of operation at these constant applied voltages. A maximum nitrate and potassium removal of 100 % and 99.82%, respectively, was obtained at 9 volts. During the electrolytic cell operation, the removal of monovalent anions was found to be higher than divalent and trivalent ones. This is different to the selectivity of monovalent and divalent cations found when use cation-exchange membrane, the removal of monovalent and divalent cations was very similar. Electrical resistance measurements showed that under constant applied voltage, anion membrane fouling decreased with increasing voltage. This is due to the mobility of anion organic molecules at high voltages. It was also found that the cation membrane fouling increased with applied voltage and that, at low voltages, the fouling was absent. It is postulated that these results from a low concentration of cation organic molecules and to the high molecular weight of this organics that limits their mobility through of solution.

RESUMEN

La remoción de nitrato y potasio de una solución de lixiviado de trigo fue estudiada usando una celda electrolítica con recirculación por tandas como procedimiento de aplicación en sistemas avanzados para soporte de vida (ALSS). Los ALSS o CELLS (Sistemas de Soporte de Vida Ecológica Controlada) son sistemas desarrollados para proveer todas las necesidades básicas humanas requeridas para misiones espaciales de largo tiempo. Altas remociones de nitrato y potasio, superiores a 90%, fueron obtenidas, a 5, 6, 7, 8 y 9 Voltios, después de 200 minutos de operación. La máxima remoción de nitrato y potasio se obtuvo a 9 voltios, 100% y 99.82% respectivamente. Durante la operación de la celda electrolítica, se encontró que la remoción de aniones monovalentes fue más alta que la de aniones divalentes y trivalentes. Esto es diferente a la selectividad obtenida en la membrana catiónica usada, la remoción de los cationes monovalente y divalente fue similar. Las medidas de resistencia eléctrica muestran que bajo voltaje constante aplicado, el ensuciamiento o "fouling" de la membrana aniónica disminuye con el aumento de voltaje. Esto es debido a la alta movilidad de las moléculas orgánicas aniónicas a altos voltajes. Se encontró que el ensuciamiento de la membrana catiónica aumenta con el aumento del voltaje aplicado, además, se observó que a voltajes bajos, no existe ensuciamiento en la membrana catiónica. Se postula que esto resulta como consecuencia a una baja concentración de moléculas orgánicas catiónicas y a un alto peso molecular de estos compuestos orgánicos, lo que limita su movilidad a través de la solución.

Master's Thesis of María Teresa Acevedo Morantes
University of Puerto Rico, Mayagüez Campus

Copyright © 2004 by María Teresa Acevedo Morantes. All rights reserved.
Printed in the United States of America. Except as permitted under the United
Copyright Act of 1976, no part of this publication may be reproduced or
distributed in any form or by any means, or stored in a data base or retrieval
system, without the prior written permission of the publisher.

This thesis is dedicated to my mother Teresa Morantes for her entirety, my father, Orlando, my brother, Edwin, my sister, Claudia, my Husband, Alvaro and especially to my Sons, Valentina and Marco Antonio.

Acknowledgements

Special mention to the people who made this work possible in one way or another.

God

NASA

Dr. Guillermo Colón

Dr. Ingrid Padilla

Mr. Ángel Zapata

Graduate Students:

Ms. Nilda Gordils

Eng. Cecilia Hernandez

Ms. Maria Curet

Mr. Alvaro Realpe

Undergraduate Students

TABLE OF CONTENTS

LIST OF FIGURES	viii
LIST OF TABLES	x
CHAPTER 1: INTRODUCTION	1
CHAPTER 2: PREVIOUS WORK	4
CHAPTER 3: MATERIALS AND METHODS	20
3.1 Objectives	20
3.2 Equipment	20
3.2.1 Fouling with and without the application of voltage	20
3.2.2 Electrolytic Cell	21
3.3 Membranes	24
3.4 Chemicals and Compartment Solutions	24
3.5 Performance of experiments	25
3.5.1 Fouling with and without the application of voltage	25
3.5.2 Batch-Recirculation Mode at Constant Applied Voltage	26
3.6 Analysis Techniques	28
CHAPTER 4: RESULTS AND DISCUSSION	29
4.1 Compartment Solutions Properties	29
4.2 Current Density	30
4.3 Electrical Conductivity of Concentrate and Dilute Strams	33
4.4 pH of Concentrate and Dilute Streams	37
4.5 Total Organic Carbon	38
4.6 Removal of Ions from Dilute Stream	41
4.7 Anions at Nitric Acid Solution	50
4.8 Fouling Results	51
4.9 Generation of Nitrogen and Oxygen	54
4.10 Normality of Nitric Acid	57
CHAPTER 5: CONCLUSIONS	60
BIBLIOGRAPHY	62

LIST OF FIGURES

Figure 1.	Schematic of a simple CELSS	5
Figure 2.	Ussing Chamber with Voltmeter.	21
Figure 3.	Four-Compartments Electrolytic cell.	22
Figure 4.	Configuration of Electrolytic Cell.	24
Figure 5.	Squematic for the batch-operation mode.. . . .	27
Figure 6.	Average current density versus time for batch operation mode.	31
Figure 7.	Initial rate of current density as function of the constant applied voltage.	32
Figure 8.	Electrical conductivity for wheat leachate as function of time at constant applied voltage.	34
Figure 9.	Initial rate of electrical conductivity from wheat leachate as function of applied voltages.	35
Figure 10.	Electrical conductivity of nitric acid at applied voltages.	36
Figure 11.	Initial electrical conductivity rate from nitric acid as function of the applied voltage.	36
Figure 12.	pH versus time of wheat leachate at constant applied voltages.	37
Figure 13.	pH of nitric acid at different constant applied voltages.	38
Figure 14.	TOC of wheat leachate as function of time at constant applied voltage.	40
Figure 15.	Initial TOC rate as function of the applied voltage.	40
Figure 16.	Nitrate removal from wheat leachate as function of time at constant applied voltage.	42
Figure 17.	Initial rate of nitrate removal as function of the applied voltage.	43
Figure 18.	Potassium removal from wheat leachate as function of the time at constant applied voltage.	45

Figure 19.	Initial rate of potassium removal as a function of the applied voltage.	46
Figure 20.	Anions Removals as a function of time at constant applied voltages.	47
Figure 21.	Initial Rate of Nitrate Concentration as a function of applied voltage.	48
Figure 22.	Cations Removals as a function of time at constant applied voltages.	49
Figure 23.	Anions Chart from nitric acid at 5 volts.	50
Figure 24.	Anions Chart from nitric acid at 9 volts.	50
Figure 25.	Resistance of the anion-exchange membrane and wheat leachate solution.	53
Figure 26.	Resistance of the cation-exchange membrane and wheat leachate solution.	54
Figure 27.	Production of oxygen as a function of time at constant applied voltages.	55
Figure 28.	Production of hydrogen as a function of time at constant applied voltage.	56
Figure 29.	Normality of nitric acid as a function of time at constant applied voltage for batch operation.	57
Figure 30.	Normality of potassium hydroxide as a function of time at constant applied voltages.	58

LIST OF TABLES

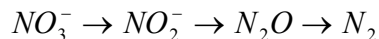
Table 1.	Properties of the electrode solutions.	29
Table 2.	Properties of concentrate solution.	29
Table 3.	Properties of wheat leachate.	29
Table 4.	Ion Concentration on wheat leachate.	30
Table 5.	Initial Current Density at different applied voltages.	32
Table 6.	Final electrical conductivity and initial rate of electrical conductivity for applied voltages.	34
Table 7.	Initial and final pH of wheat leachate.	38
Table 8.	Decrease of TOC and initial TOC rate at applied voltage.	41
Table 9.	Nitrate removal and initial nitrate removal rate at constant applied voltages.	42
Table 10.	Potassium removal and initial potassium removal rate at constant applied voltages.	45
Table 11.	Initial rate of nitrate concentration at applied voltages.	48
Table 12.	Final membrane resistance of anion membrane and initial fluid electrical resistance	52
Table 13.	Final membrane resistance of cation membrane and initial fluid electrical resistance	53
Table 14.	Final and Total production of oxygen and hydrogen at batch processes.	56
Table 15.	Normality of nitric acid at constant applied voltage.	58
Table 16.	Normality of potassium hydroxide at constant applied voltage.	59

CHAPTER I

INTRODUCTION

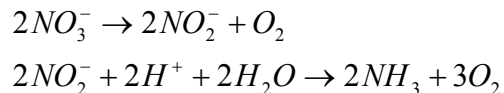
The National Aeronautical and Space Administration (NASA) has developed a controlled Ecological Life Support System (CELSS) to provide all the basic human needs required for long-term space missions. This project, CELSS, has two main phases or stages: the Biomass Production Chamber (BPC) and the Resource Recovery System (RRS).

The BPC produces oxygen, edible and inedible products, and water from hydroponics crops. The RRS processes inedible products and/or residues crop using aerobic and anaerobic bioreactors to recover plants nutrients and secondary foods. The inedible products are treated in a process of water extraction or leaching to remove nutrient prior to further treatment in the bioreactors. Leaching is effective at removing the majority of nutrients from the inedible biomass. The aqueous leachate contains both inorganic and organic molecules, as inorganic molecules were found nitrate, phosphate, sulphate, chloride, potassium, magnesium and calcium, between others. The high concentration of nitrate in aqueous leachate causes serious problems in the anaerobic and aerobic bioreactors: nitrogen losses through denitrification in the aerobic biodegradation and conversion of nitrate to ammonia during the anaerobic process. The denitrification is a reduction reaction where nitrates are reduced, and produce N_2 gas as the end product, as shown in the following reaction (Mackie, 2001):



The nitrogen produce in this process is available for biological nitrogen fixation. The microorganisms consume the oxygen and prevent nitrogen from entering their cells. There is an oxygen demand exerted, which can have negative effects on the dissolution of organic matter in aerobic reactors, decreasing the efficiency the aerobic degradation.

In anoxic conditions the bacterial action on organic matter, releases nitrate, which may be reduced to nitrite and reduced additionally to ammonia. These reactions are as follows:



The recovery of nitrate from leachate of biomass is an alternative to avoid these difficulties in the bioreactors, and to produce nitric acid that is used to control the pH in the aerobic bioreactors. The aerobic decomposition of organic compounds increases the pH in these bioreactors and affects efficiency.

Electrodialysis (ED) is an effective process to remove nitrate ions from waste and leachate of biomass. ED is an ion exchange membrane separation process that uses an electrical potential as a driving force. This technology does not require chemicals and is simple to operate. It adapts to non-continuous feed supplies and different loads. Besides, it is not very dependent on temperature

and it has a recovery rate of more than 97%. All these characteristics make electrodialysis an especially attractive method, to remove nitrate from leachate of biomass in CELSS, both ecologically and economically.

In spite of the advantages of ED, fouling of ion exchange membranes may limit the design and operation of ED processes. Fouling is essentially caused by deposition of foulants on the membrane surface, causing deterioration in the membrane performance, in terms of flux decline and increase in the electrical resistance. Besides, the fouling sometimes causes a loss in selectivity of the membrane. If the fouling is irreversible, the membranes must be changed frequently, adding to the increased energy cost caused by fouling.

The purpose of this work is:

- 1) To determine the effect of applied voltage about the membrane electrical resistance (fouling) of Electrolytic process. Moreover,
- 2) To study the fouling effect on the efficiency of ED processes and,
- 3) To determine the removal rate of nitrate and potassium.

CHAPTER 2

PREVIOUS WORK

Electrodialysis (ED) and electrolytic (EC) processes are ion exchange separation methods considered as the next leading separation techniques in industrial process. ED and EC processes have several advantages about other methods of removal:

- These methods do not require chemicals and are simple to operate.
- They adapt immediately to non-continuous process and different loads
- Temperature changes have a negligible effect on these processes.
- They have high recovery rate of more than 97%.

These advantages make electrodialysis and electrolytic processes attractive for environmental and biotechnological applications as well as in the production of table salt and the desalination of seawater. The nitrate removal from ground and surface water is an environmental application of ED (Elmidaoui et al. 2001). This removal can be leading by degradation and separation processes. But, the high selectivity and low chemical demand are advantages that position the ED above others removal options.

There is a special interest to separate the nitrate from drinking water, ground water, and inedible biomass leachate. The nitrate removal from inedible biomass leachate is a useful process in the project of Controlled Ecological Life Support

System (CELSS), as is explained in page 6. The mission of project CELSS, as bioregenerative life support system, is to perform all the basic functions of a life support system based on a natural cycle regenerative process (Figure 1). The CELSS concept is that a human life support system, supplying food, water, and oxygen, open with respect to energy but closed with respect to mass, can operate indefinitely in space without resupply from Earth. This system, also known as ALSS (Advanced Life Support System), incorporates biological components in the synthesis, purification, and regeneration of basic life support in future space missions. CELSS will provide basic and continuous life-support requirements such as food, drinking water, cleaning water, and breathable atmosphere, by using plants as the central recycling component for waste.

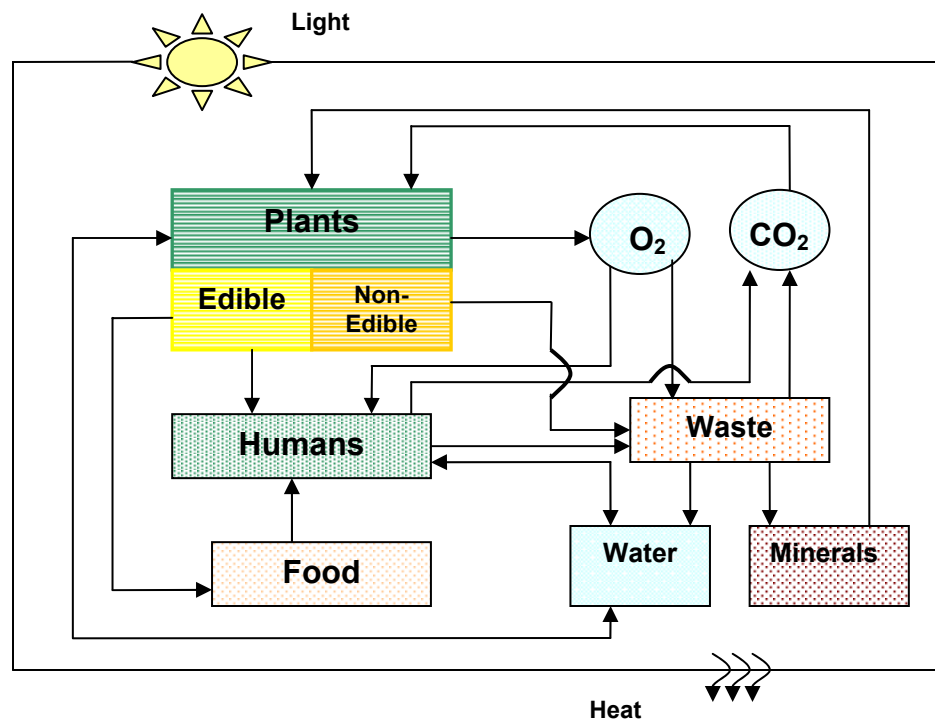


Figure 1. Schematic of a simple CELSS showing major components and flows

One main purpose of the CELSS is to recycle inedible material into carbon dioxide and mineral forms that can be used by crops and to convert these inedibles into food. During this process, the biodegradable inedible crop residues (stems, leaves, roots, chaff/pods, etc) are decomposed in anaerobic and aerobic bioreactors. The major products of aerobic decomposition are (1) carbon dioxide and inorganic forms of mineral elements, which must be recycled for further plants growth, and (2) microbial biomass production. The major products of anaerobic decomposition are (1) carbon dioxide and (2) volatile fatty acids (acetic, propionic, butyric, etc).

The soluble extract from inedible biomass can be used as a plant nutrient source in hydroponic systems (Garland and Mackowiack, 1990; Garland et al., 1993). Leaching process of inedible biomass is effective at removing the majority of nutrients from the inedible biomass, although addition of inorganic nutrients has been necessary in some cases (Garland 1992). The aqueous leachate contains both inorganic and organic molecules. Biological processes of leachate have been used previously to reduce the concentration of organic molecules in the leachate, convert soluble organic to edible products, therefore, reduce phytotoxic effects in hydroponic culture (Garland, 1992). The significant amount of nitrate contained in the inedible crop residues leachate, however, causes undesirable results in the aerobic and anaerobic bioreactors: nitrogen losses through denitrification in the aerobic biodegradation and conversion of nitrate to ammonia during the anaerobic process. The aerobic denitrification

process consumes part of the medium dissolved oxygen, which is required to solubilize the organic matter present. Furthermore, the produced nitrogen gas is not an important compound needed in the CELSS. The anaerobic decomposition of nitrate to ammonia demand further nitrification process, to convert the ammonia to nitrate to use as plant nutrient, which require additional oxygen in the process. In, addition, the aerobic decomposition of organic compounds in crop leachate, result in an increase of pH increased from 6.5 to 8.5 disturbing the microbial populated (Finger et al. 1994). Research has used a 1N nitric acid solution to control the pH during crop residues decomposition. Hence, it is suggested to remove nitrate prior to the decomposition process and to use it for the production of nitric acid.

Nitrate contamination is increasingly due to widespread use of fertilizers containing nitrate and from poorly or untreated human and animal wastes. There are two major concerns with elevated nitrate levels including Cultural or anthropogenic eutrophication in lakes and human health. Cultural or anthropogenic "eutrophication" is water pollution caused by excessive plant nutrients (primarily phosphorus, nitrogen, and carbon). These substances can overstimulate the growth of algae, creating conditions that interfere with the recreational use of lakes and estuaries, and the health and diversity of indigenous fish, plant, and animal populations.

Algal blooms hurt the system in two ways. First, they cloud the water and block sunlight, causing underwater grasses to die. Because these grasses

provide food and shelter for aquatic creatures (such as the blue crab and summer flounder), spawning and nursery habitat is destroyed and waterfowl have less to eat when grasses die off. Second, when the algae die and decompose, oxygen is used up. Dissolved oxygen in the water is essential to most organisms living in the water, such as fish and crabs.

The major concern affecting human health pertains to infants less than six months of age. In sufficient quantities, at nitrate concentrations exceeding 10 mg/L, the possibility of a health hazard is significant towards infants. This health hazard is due to a bacterium that exists in their gastrointestinal tract that converts nitrate to nitrite (NO_2). The nitrite produced then reacts with hemoglobin to form methemoglobin, which does not carry oxygen. Consequently the infant receives less oxygen to the brain, resulting in slate blue skin, vomiting, diarrhea, mental retardation and/or suffocation leading to death. This is a syndrome known as methemoglobinemia or “blue baby” syndrome. After six months of age nitrate is absorbed and secreted without conversion to toxic nitrite. Besides, there is evidence that other health problems are associated with nitrate including stomach cancer, birth defects, hypertension, enlarged thyroid and lymphoma. (Fonseca et al., 2000; Dorsheimer et al., 1997)

Nitrate is a stable and highly soluble ion and has a low potential for adsorption or coprecipitation. These properties are what make this ion difficult to remove using conventional water treatment processes including lime softening and filtration. The removal options are reverse osmosis, ion exchange,

biological denitrification, ion exchange bioreactor, catalytic reduction, chemical denitrification and electro dialysis.

Electrodialysis is an electromembrane process used widely, especially for desalination of brackish water and sodium chloride reconcentration from seawater. It has been widely applied for production of table salt, organic acids, remediation of heavy metal polluted soil, sugar demineralization, blood treatment, and wine stabilization. ED is also an important membrane processes for environmentally clean technology in biotechnology industries. Recovery of various acids by ED has been reported, including sulfuric acid (Cattoir et al., 1999; Urano et al., 1984), hydrochloric acid (Shah and Scamehorn, 1987; Urano et al., 1984), phosphoric acid (Hanley et al., 1986), nitric acid (Colon et al., 2001); tartaric acid (Andres et al., 1997) and lactic acid (Kim et al., 2001; Colon et al., 1987).

The nitrate recovery using electro dialysis has been developed by several researchers. Elmidaoui, et al., 2001, tested five types of anion exchange membranes (AFN, ACS, AMX, ADP and ADS) and one type of standard cation exchange membrane (CMX membrane) in a electro dialysis cell to select the best anion exchange membrane for nitrate removal, and study the nitrate removal by electro dialysis in a electro dialysis pilot. The obtained results of the variations of nitrate rejection and of the sulfate rejection with overall rejection for all the tested membranes show that the best behavior in nitrate removal by electro dialysis was obtained with the ACS membrane. The NEOSEPTA ACS monoanion

permselective membrane has excellent nitrate selectivity. The electro dialysis was carried out in the electro dialysis pilot cell equipped with a CMX membrane (standard cationic ion exchange membrane) and an ACS membrane (mono-anion permselective membrane). To control the permselectivity of the ACS membrane, an electro dialysis operation was carried out in an aqueous solution containing a sodium salt mixture at concentrations of 500 ppm of each anion: $\text{NaCl} + \text{Na}_2\text{SO}_4 + \text{NaNO}_3 + \text{NaHCO}_3$. At conditions of 20°C, voltage 15 V and flow rate 180 l/h, the results showed the simplicity to conduct the electro dialysis process in comparison with the conventional denitrification processes. Chemical and spare parts cost are not significant. The membrane replacement and electricity constitute the greater part of the operating cost. The investment increase when capacity of the plant decrease and/or the required nitrate removal is superior to 80%.

Eyal and Kendem (1988) have attempted to bring out selectivity for the elimination of nitrates during electro dialysis by the introduction of polyfunctional groups in an anion exchange membrane. Kesore et al. (1997) used an anion exchange membrane coupled with a new intermembrane spacer containing a nitrate-selectivity anion exchange resin to improve the selectivity and effectiveness of nitrate removal from drinking water. The modified membrane to monovalent anions, allows the arriving sulphates to be transported only at a second position after the nitrates. Therefore, the active spacer intensifies the mass-transfer process as a whole, implying a deeper desalination of the feed.

Permselective membranes for ED contain either groups of positive ions (anion-exchange membranes) or negative ions (cation-exchange membranes). In an applied electric field and in aqueous solution, an anion-exchange membrane permits the passage of anions only; a cation exchange membrane permits the passage of cations only. The most important characteristics of permselective membranes used for ED are: low electrical resistance, good permselective qualities for cations or anions, good mechanical properties, good form stability, and high chemical stability. It is difficult to find all of these properties together in the commercially produced membranes.

There are two types of membranes: heterogeneous and homogeneous (Curet, 2000 and Korngold, 1984). The heterogeneous membranes are manufactured by mixing a commercial ion exchanger with a solution of binder polymer, such as polyvinyl chloride (PVC), rubber, or polyvinylidene fluoride. The membrane polarity is determined by the ion exchanger. The ion exchangers used in ED membranes are usually made of a copolymer of styrene and divinylbenzene (DVB). The cation-exchange group is introduced into the copolymer by sulfonation with concentrated sulfuric acid at 60-90 °C. The anion-exchange group is introduced into the polymer by chloromethylation and amination with a triamine (such as $(\text{CH}_3)_3\text{N}$).

The homogeneous membranes consist of a continuous homogeneous film into which an active group (cationic or anionic) is introduced. Graft copolymer of styrene in a polyethylene film is used to produce homogeneous membrane. Another method of producing homogeneous membranes is by the

sulfochlorination of a polyethylene film, an active group SO_2Cl is bound to the polyethylene film. A cation-exchange membrane is then obtained by hydrolysis and the anion-exchange membrane by amination and quaternization.

Cherif et al., 1997, used and compared three cell configurations with three or two compartment cells with anion or cation exchange membranes (CEM) in stack series to produce HNO_3 and NaOH from NaNO_3 , which can be found in industrial waste waters. The membranes were bipolar membranes (BPM), which are composed of an anion exchange layer, a cation exchange layer and a hydrophilic interface at the junction of the two layers. In this hydrophilic interface, water molecules are split into protons and hydroxide ions. This process allows the use of electrodialysis to improve the recovery of acids and bases from their salts. This research showed best results using the cell with three compartments; the two compartment system cannot work to produce nitric acid because of the deprotonation of vinyl pyridinium groups inside the AEM with increasing concentration of hydroxide ions. This last process are used to obtain acids or bases with relative assay because operate with low energy requirement.

Colon and Sager (2001) reported electrolytic removal of nitrate from crop residues using a four-compartment electrolytic cell (EC) at 4.5 and 8.5 V. They considered process variables, such as limiting current density, applied voltage and fluid velocity, between others. The ions removal rates were proportional to the current density, the ions concentration, operating time and the mobility in solution of ions, inversely proportional to fluid velocity and independent of applied voltage. In the electrolytic cell, as electrodialysis, there are electrodes at each

end that provide the current that flows through the compartments or cells in series. Alternating cation exchange and anion exchange membranes are used to separate the compartments, forming a repeating cell-pair pattern (positive and negative). One cell in each pair contains a concentrated solution and the other contains a dilute solution. The electrically charged membranes and the electrical potential difference are used to separate ionic species from dilute solution compartment to the concentrated solution compartment. EC is a process for separating low molecular weight electrolytes from solutions (Korngold, 1984 and Flett, 1983). The difference between an electrolytic and an electro dialysis cell is the configuration of the cell. In electro dialysis, cation and anion exchange membranes are alternated between two electrodes and a repeated cell-pair pattern can be formed, thus several cell pairs can be assembled between the electrodes. In the case of an electrolytic cell unit, the addition of cell pairs requires the addition of electrodes (Curet, 2000).

Mass transfer through permselective membranes consists of two steps: The reduction of salt concentration in the solution by electrotransport of ions from the boundary layer near the membrane, and the diffusion of ions to the partially desalinated boundary layer.

The kinetics of the first step is given by the Nernst equation

$$J_e = (\bar{t}_m - t_s) i / F \quad (1)$$

Where J_e is the flux of ions by electrotransport, i the current density, F the Faraday number, t_s the transport number in solution, and \bar{t}_m the transport number in membrane.

The second step is given by Fick's First law:

$$J_D = D(C - C_0) / \delta \quad (2)$$

Where J_D is the flux of ions by diffusion, D the diffusion coefficient, C the concentration of the solution, C_0 the concentration of the solution at the boundary layer, and δ the thickness of the boundary layer. The thickness of the boundary layer δ is a function of the linear velocity of the solution in the cell and the geometry of the spacer.

Under steady state conditions:

$$J_e = J_D \quad (3)$$

From Eqs. (1) and (2), the following can be derived:

$$i = \frac{DF(C - C_0)}{\delta(\bar{t}_m - t_s)} \quad (4)$$

This equation shows that increasing the voltage of the stack raises the current density. The flux of ions by electrotransport is also increased until the concentration of the solution in the boundary layer approaches zero ($C_0 \approx 0$).

Under these conditions the flux of ions by diffusion is at maximum:

$$J_{D(\max)} = DC / \delta \quad (5)$$

and

$$i_{(\max)} = DFC / \delta(\bar{t}_m - t_s) \quad (6)$$

A further increase in J_D can be achieved only by decreasing δ . This can be achieved by raising the linear velocity of the solution in the cell to a level at which the pressure drop across the cells will not cause internal leakage.

When

$$J_e = J_{D(\max)} \quad (7)$$

the ED unit is operating at the highest value of mass transfer. A further increase in the stack voltage will raise the current density. Most of this additional current, however, will cause dissociation of water rather than mass transfer from the diluate to the concentrated cells (Korngold, 1984).

When the concentration of the solution in the boundary layers decreases, the electrical resistance of the cell pair increases. When the concentration in the boundary layers is low, the water dissociates, causing scaling and fouling on the anion-exchange membranes. Therefore, it is important that the current density be prevented from approaching the limiting current-density value. This value can be obtained by plotting cell-pair resistance versus current density. A practical equation has been suggested for limiting current density, (Korngold, 1984):

$$\frac{i_{\text{lim}}}{C_{\text{av}}} = KU^b \quad (8)$$

Where U is the linear solution velocity in stack, K an empirical number, generally between 50 and 200, b an empirical number generally between 0.5 and 0.9, and C_{av} is the average concentration as expressed in the following equation:

$$C_{\text{av}} = \frac{C_1 - C_2}{2.3 \log(C_1 / C_2)} \quad (9)$$

Equation (8) can be approximated by (Maurel, 1972)

$$i / C_{\text{av}} = 145U^{0.6} \quad (10)$$

In the research developed by Curet (2000), the limiting current density (LCD) was obtained performing experiments at once-through continuous operation for different fluid velocities and leachate ionic concentrations. The applied voltage was monitored as a function of electrical current density and the limiting current density was obtained for five fluid velocities and at four leachate dilution ratios. The optimal current density is a function of the water concentration. A correlation between limiting current density, fluid velocity, U , and dilution ratio, C^* , was established:

$$i_{\text{lim}} = \alpha U^B C^* \quad (11)$$

Where α is a constant with a value of 497.4 A/m^2 , this value was obtained for an electrolytic cell with the specifications of chapter 3. The function correlation at non-diluted leachate was obtained and is the following:

$$i_{\text{lim}} = 492.5U^{0.7012} \quad (12)$$

Material balances in an electrolytic cell continuous mode of operation can be obtained by (4):

$$\ln \frac{N_f}{N_p} = \left[\left(\frac{e}{F} \right) \left(\frac{i}{N_d} \right) \left(\frac{A_m}{Q} \right) \right] \quad (13)$$

Values of (i/N_d) and A_m may be chosen from an empirically determined relationship between (i/N_d) and the fluid velocity. For batch-recirculation operation mode in electrolytic cell, it is apparent that multiple passes through a single stack are equivalent as to passing the solution through several stacks in series. The performance equation for a batch recirculation process is as follow:

$$\frac{N_f}{N_{nm}} = \exp \left(\frac{A_m}{FQ} \sum_{k=1}^n \left(\frac{i}{N_d} \right)_k e_k \right) \quad (14)$$

If the process is carried out at constant average value of $(i/N_d)_{av}$ and assuming an average current efficiency, e_{av} , Eq. (14) can be simplified to:

$$\ln \frac{N_f}{N_{pn}} = \left[\left(\frac{ne_{av}}{F} \right) \left(\frac{i}{N_d} \right)_{av} \left(\frac{A_m}{Q} \right) \right] \quad (15)$$

The value of $(i/N_d)_{av}$ may be simulated partially by operating at a constant voltage determined empirically from polarization studies.

Fouling of permselective membranes is one of the most important limitations in the design and operation of an ED process. Fouling is essentially caused by deposition of foulants on the membrane surface, causing deterioration in the membrane performance, in terms of a decline in the flux and an increase in the resistance (Lee et al., 2002 and Korngold, 1984). Fouling can be of three types:

- Organic anions that are too large to penetrate the membrane and accumulate on its surface. Mechanical cleaning can restore the original electrical resistance of the membrane. Therefore this type of fouling can be prevented by filtering the solutions, and using tortuous flow path spacers and high fluid velocities.
- Organic anions that are small enough to penetrate the membranes but whose electromobility is so low that they remain inside the membrane, causing considerable increase of resistance. Different kinds of tensio-active agents can cause this type of poisoning, and it is difficult to restore the original electrical resistance of membranes poisoned in this way.
- Organic anions that are smaller than those of previous category, but still cause a certain increase in electrical resistance of the membrane. These anions can be eluted by electroelution with sodium chloride, and the original properties of the membrane can be obtained.

Since most of the colloids present in natural water are negatively charged, it is almost always the anionic membranes which are affected by fouling. Fouling due to negatively charged organics occurs in many streams of ED application, some of the foulants being sodium dodecylbenzene sulfonate, sulfonated lignin, sodium humate, grape must and milk whey. Negatively charged organic foulants move toward anion exchange membranes under an electric field and deposit on the surface of membranes due to electrical interactions between the membrane surface and the foulants. The physical parameters of the solute that influence fouling on and in the membrane include: charge, hydrophobicity, molecular size and solubility. Precipitation in and on the membrane is governed by the solubility of the solute, and the adsorption is affected by electrostatic and hydrophobic interactions between the solute and the membrane surface. Electrostatic interactions depend on the charge of the molecule and the membrane. The size of the molecule also affects the solubility, and hence, the probability of precipitation on and in the membrane. The concentration of the solution also affects the membrane resistance. A marked increase in fouling was observed when approaching the saturation concentration (Lindstrand et al., 2000).

CHAPTER 3

MATERIAL AND METHODS

3.1 Objectives

The development of experiments was fixed in the determination of fouling effect about electrolytic process. To study the effect of applied voltage on membrane electrical resistance and efficiency of EC processes were the main objectives of this research.

3.2 Equipment

3.2.1 Fouling with and without the application of voltage

Experiments were performed in an Ussing chamber that is conformed by two halves (Figure 2). The volume of each chamber is approximately $5 \times 10^{-7} \text{ m}^3$ and the area of each electrode $1 \times 10^{-5} \text{ m}^2$. The Ussing chamber has eight ports and is made of acrylic. The four ports on top of the chamber are connected to the solution reservoir, as shown in Figure 2. Opposed 90 degrees to the four connectors in the middle of the Ussing chamber two ports for the voltage electrodes; on the opposite side and near each end of the chamber are two ports for current electrodes. The electrodes are connected to a voltmeter and ammeter with current/voltage (I/V) clamp capabilities (DVC-1000 Dual Voltage Clamp, World Precision Instruments, Inc, Sarasota, FL).

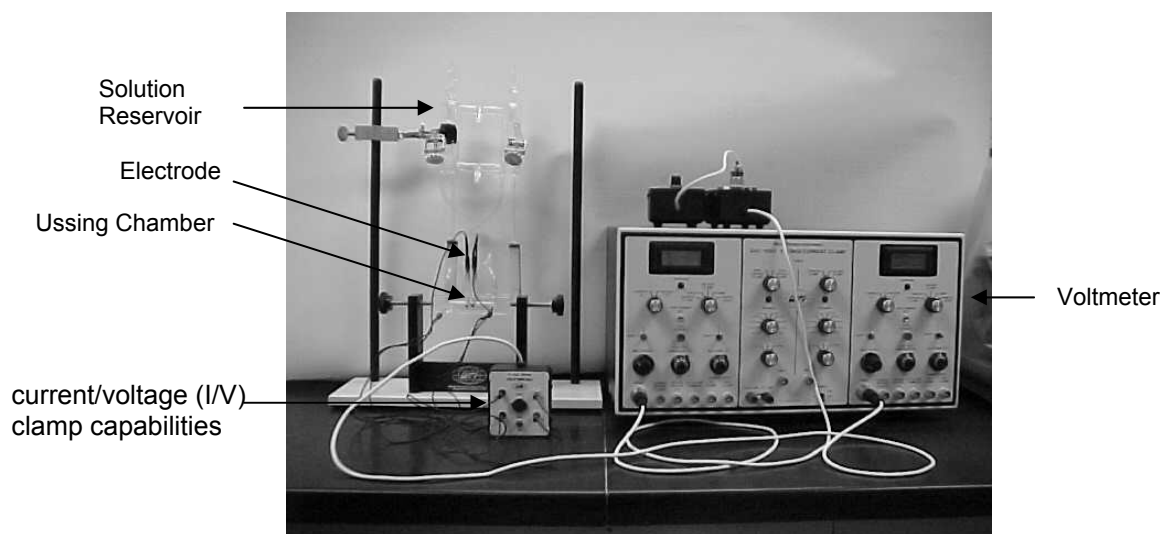


Figure 2. Ussing Chamber with Voltmeter (DVC-1000 Dual Voltage Clamp, World Precision Instruments, Inc., Sarasota, FL)

3.2.2 Electrolytic Cell

Experiments were performed in an electrolytic cell (EC), which consists of four compartments with dimensions of $0.23\text{m} \times 0.25\text{m}$, two heavy duty cation-selective membranes (type CR64 LMP-447, IONICS, Inc., Watertown, MA) and one anion-selective membrane (type 204-SZRA-412, IONICS, Inc. Watertown, MA) (see Figure 3). The effective membrane area is 0.023 m^2 and the thickness of the spacer between the membranes is 2.2 mm and 1 mm. The spacers are made of propylene and manufactured by IONICS, Inc., US. The separation between electrodes and cation membranes was done with propylene tortuous path spacers with a cross sectional area for the flow of the spacers is $1.2 \times 10^{-5}\text{ m}^2$. The two propylene tortuous path spacers for the concentrate and the dilute streams have a cross sectional area of $6 \times 10^{-6}\text{ m}^2$. The anode is a titanium

substrate platinum plated electrode and the cathode is stainless steel (Figure 3). The EC were connected to a DC power supply (Series 3000, Power Ten, Inc., California, US), which can supply different currents and voltages. pH electrode (model 62398 from Omega) and an electrical conductivity flow meter (1481-60, 500 series from Cole Parmer) were installed at the inlet of the wheat leachate. Solutions were recirculated through the electrolytic cell by means of a pumps (Cole Parmer Instruments Model No.7520-00, 3 A, 115 VAC, 50/60 Hz) and the flows were measured using two digital flow meters (111Flo-meter, McMillan Co.).

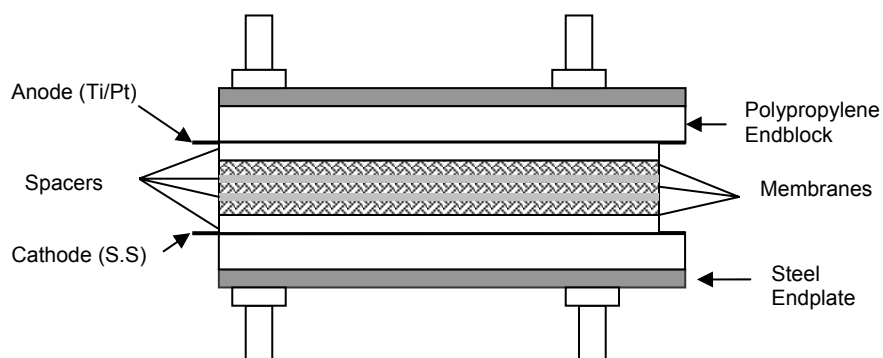


Figure 3. Four-Compartment Electrolytic Cell

In an EC the solutions flow in an upward direction, and a direct electrical potential is applied perpendicular to the solutions. The solutions that were used are potassium hydroxide and sulfuric acid as electrode solutions, and nitric acid and wheat leachate as concentrated and dilute solutions, respectively.

When an electrical potential is applied to the electrolytic cell, in the dilute solution, potassium ions and other cations move to the cathode, while nitrate ions and other anions move to the anode. Hydroxide ions are obtained by water electrolysis; these ions are then combined with potassium ions at the cathode compartment to produce potassium hydroxide. The electrolytic reduction of water also produces hydrogen gas, which may be used as a potential fuel. The nitrate ions removed from the leachate compartment pass through the anion-exchange membrane to the nitric acid compartment. At the nitric acid compartment, the nitrate ions combine with the hydrogen ions that come from the anode compartment; this results in an enrichment of the nitric acid solution. At the anode compartment, water oxidizes under acid conditions and produces oxygen gas and hydrogen ions. As a result, oxygen, hydrogen and nitric acid are produced in this electrolytic process (Figure 4).

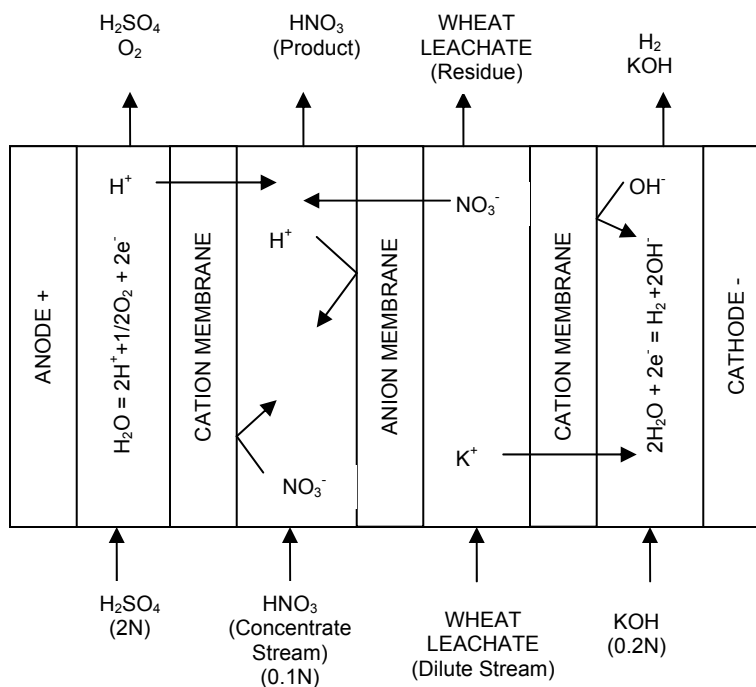


Figure 4. Configuration of Electrolytic Cell

3.3 Membranes

An anion-selective membrane (type 204-SZRA-412, IONICS, Inc. Watertown, MA) and a cation-selective membrane (type CR64 LMP-447, IONICS, Inc., Watertown, MA) were used in the investigation. The cation membrane and anion membrane are based on polypropylene and copolymer of methyl acrylate and acrylonitrile respectively.

3.4 Chemicals and Compartment Solutions

KCl solution 1 M was used to measure the resistance of membranes and as a reference electrolyte. Leachate wheat was used as foulant solution. The

leachate wheat was obtained by leaching. The extraction of nutrients from the inedible wheat biomass was carried out following the procedure described by Garland and Mackowiak (1990). Leaching was performed in a cylindrical vessel containing a 200 μm mesh above the drain valve to remove the suspended matter that may clog the electrolytic cell. The loading was 50 g biomass per liter of distilled water. The biomass consisted in dry inedible wheat residues. The leaching was done in a batch of 500 g with aeration for two hours. The biomass was rinsed with an equal amount of distilled water in a separate wash for 15 minutes. The wheat leachate was filtered with a 12 μm and 0.45 μm filters from Santorius, Inc.

The concentrate stream was a nitric acid solution of 0.1 N, and the feed solution for the cathode compartment was a 0.2 N Potassium Hydroxide. These concentrations were chosen to keep the ratio of electrical conductivities of these solutions to the leachate solution below 10 in order to prevent back diffusion. The feed solution for the anode compartment was a 2 N Sulfuric Acid.

3.5 Performance of experiments

3.5.1 Fouling with and without the application of voltage

Previously unused membrane samples were used in all tests. The area of each membrane was $5.1 \times 10^{-4} \text{ m}^2$. Before the experiments the membranes were stored in deionized water to avoid shrinkage. The solution used in all experiments was a sample of biomass leachate (wheat leachate) at the same conditions of the solution used in the EC. The membrane sample was fixed in

the resistance-measuring equipment (Ussing Chamber), and the electrical resistance of the solution plus the electrical resistance of the membrane, R , were registered. Inrush time, membrane electrical resistance was measure every 5 minutes to estimate the fouling by the organic substance. The chambers were opened and the membrane was removed, and the measurement was repeated without the membrane. The electrical resistance of the membrane was calculated as the difference between the readings with and without the membrane.

$$R_m = R - R_{sln} \quad (16)$$

The fouling was determined as the increase in resistance with the time with 0, 25, 50, 75 and 100 mV.

3.5.2 Batch-Recirculation Mode at Constant Applied Voltage

The schematic for the batch-recirculation operation mode is shown in Figure 5. The solutions for batch-recirculation mode were 4.5 L of wheat leachate and 0.1 N nitric acid. The electrode solutions contained 9 liter of 2 N sulfuric acid and 0.2 N potassium hydroxide. The solutions were kept well mixed in containers via magnetic stirred agitation. The solutions were recycled through the electrolytic cell. Thus, the leachate solution became diluted while the nitric acid solution became more concentrated (Figure 5).

Experiments were performed at a constant fluid velocity of 0.14 m/s in the leachate solution, and nitric acid, and 0.28 m/s in the electrode solutions. For each batch-recirculation mode experiment, the applied voltage was kept constant. Twelve experiments were performed at six different voltages: 4, 5, 6, 7, 8 and 9 Volts, and two experiments were done for each voltage. Time intervals, currents, pH and electrical conductivities of wheat leachate (dilute stream) and the temperatures of all solutions entering and leaving the were recorded. Samples of the four solutions were taken. All analyses were made as function of time and current densities. The experiments were realized with a single factor, voltage, and a replicate. Shown results are the average between the run and replicate.

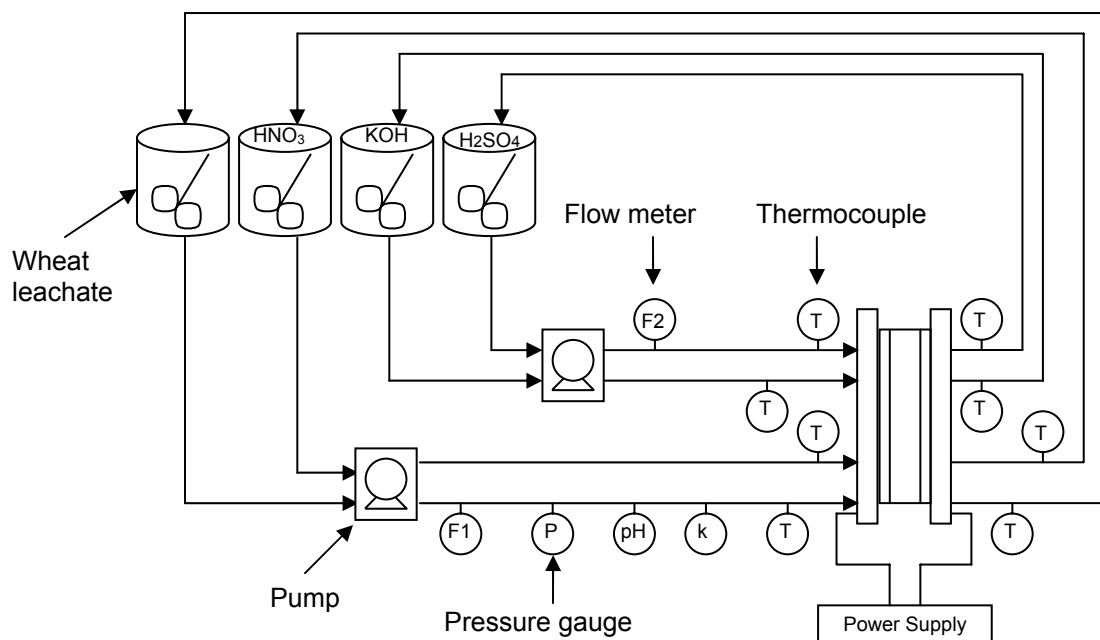


Figure 5. Schematic for the batch-operation mode.

3.6 Analysis Techniques

An ion chromatographer (766 IC Sample Processor, 753 Suppressor, 709 IC Pump, 733 IC Separation Center, 732 IC Detector from Metrohm) was used to measure the ions concentrations in solution samples. The anions concentrations were measured using a Metrohm A-Supp5 Column and the suppressor module. Suppression was reached with 100 mM sulfuric acid and deionized water. The eluent was a solution of 3.2 mM Sodium Carbonate and 1 mM Sodium Bicarbonate. The flow rate for this analysis was 1 mL/min. The cations concentrations were measured using a Metrosep Cation Column 1-2. The eluent was a solution of 4 mM Tartaric Acid with 0.75 mM dipicolinic acid (PDCA). The flow rate for this method was 1.0 mL/min. For ions analysis, the used eluents were filtered at 0.22 μm and degasified for 15 minutes. Samples had to be diluted with deionized water previous to analysis to be in range of calibration curves.

The analyses of total organic carbon (TOC) were carried out with a Total Organic Carbon Analyzer (UV Persulfate TOC analyzer, Dohrmann, Phoenix 8000). The electrical conductivity of leachate, nitric acid and potassium hydroxide samples was measured with a conductivity meter (Thermo Orion, model 150Aplus). The pH was measured with a pH electrode (model 290 A from Orion). The samples of nitric acid and sulfuric acid were titrated with 0.1 N and 2 N Sodium Hydroxide respectively to determine the normality, and the samples of potassium hydroxide were titrated with 0.2 N Hypochlorite acid.

CHAPTER 4

RESULTS AND DISCUSSION

4.1 Compartment Solutions Properties

Table 1 and 2 show the properties of the electrode solutions and concentrate stream. Table 3 and 4 show the properties and the ion composition of the wheat leachate. The relations between the potassium hydroxide conductivity, nitric acid conductivity and wheat solution conductivity are 12 and 10, respectively. It is sufficient to remove nitrate and potassium from wheat solution by electrical field using the electrolytic process.

Table 1. Properties of the electrode solutions

Electrode	Solution	pH	k (mS/cm)
Cathode	Potassium Hydroxide (0.2N)	13.098	48.2
Anode	Sulfuric Acid (2N)	0.630	170.3

Table 2. Properties of concentrate solution

Concentrate Solution	pH	k (mS/cm)	[NO₃] (ppm)
Nitric Acid 0.1 N	1.50	39.00	6362.052

Table 3. Properties of wheat leachate

Solution	pH	k (mS/cm)	TOC (ppm)
Wheat leachate	5.798	3.75	2330.45

Table 4. Ion Concentration on wheat leachate

Ion	Concentration (ppm)
Fluoride	45.499
Chloride	223.849
Phosphate	1741.220
Sulfate	1046.166
Nitrate	1442.902
Calcium	87220.5153
Magnesium	4199.864
Sodium	0.000
Ammonium	35.099
Potassium	1390.070

4.2 Current Density

The electrolytic cell has been tested in a batch-recirculation mode of operation at six constant applied voltages 4, 5, 6, 7, 8 and 9 Volts, and at a constant fluid velocity of 0.14 m/s. Cell current density, solutions electrical conductivities, pH and ions concentrations were monitored as function of time.

In electrolytic process the ions concentration of wheat leachate decreases with the time, thus the electrical resistance of the solution increased, yielding a decrease of current needed to keep the applied voltage constant (Figure 6). Figure 6 shows the current density as function of time for six constant applied voltages. The time of operation decreases slightly with higher applied voltage. Moreover the initial current density increases with the higher applied voltage. Also, it is observed that the current density decreases exponentially with the time. At applied voltages of 5, 6, 7, 8 and 9 volts, the current density behavior is the same at times higher than 200 min. At 4 volts, the current density was lower than those at 5 to 9 volts; indicating that the ions removal is the lower, at 4 volts. Table 5 shows the values of average current density, initial rate of current density, operation time and standard deviation at applied voltages. It can be

observed that there is not a significant difference between operation time at 4 and 5 Volts and 6 and 7 Volts, possibly due to same conditions in the electrolytic cell at the final of mode operation.

Figure 7 shows the initial rate of current density as function of voltage. It also shows that operation at constant applied voltage has a behavior of linear function with a slope of 2.0985, a coefficient of 11.7910 and a correlation factor (Rsqr) of 0.9984:

$$-\left. \frac{di}{dt} \right|_{t \rightarrow 0} = 11.7910 + 2.0985E$$

Where

$$\left. \frac{di}{dt} \right|_{t \rightarrow 0} = \text{Initial current density rate, [A/ m}^2 \text{ min]}$$

$$E = \text{Applied voltage, [Volts]}$$

This linear behavior corresponds to the initial cell electrical resistance as described by Ohm Law. All cell solutions initially have the same ions concentrations.

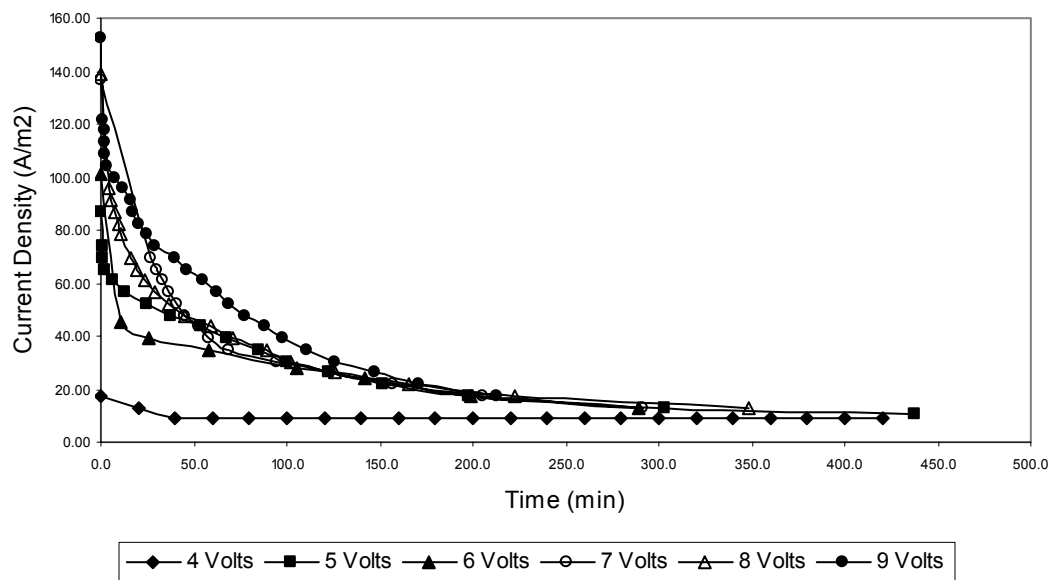


Figure. 6. Average current density versus time for batch operation mode

Table 5. Initial Current Density at different applied voltages

Voltage (Volt)	Initial Current Density (A/m ²)	$-\frac{di}{dt}\Big _{t \rightarrow 0}$ (A/m ² min)	Operation time (min)	Std. Error
4	17.39	19.8992	420.00	0.3575
5	86.95	22.365	438.135	0.8930
6	101.1	24.6078	289.00	2.2008
7	137.0	26.67717	291.50	1.0444
8	139.13	28.6099	348.00	1.5320
9	152.17	30.4278	304.50	1.5232

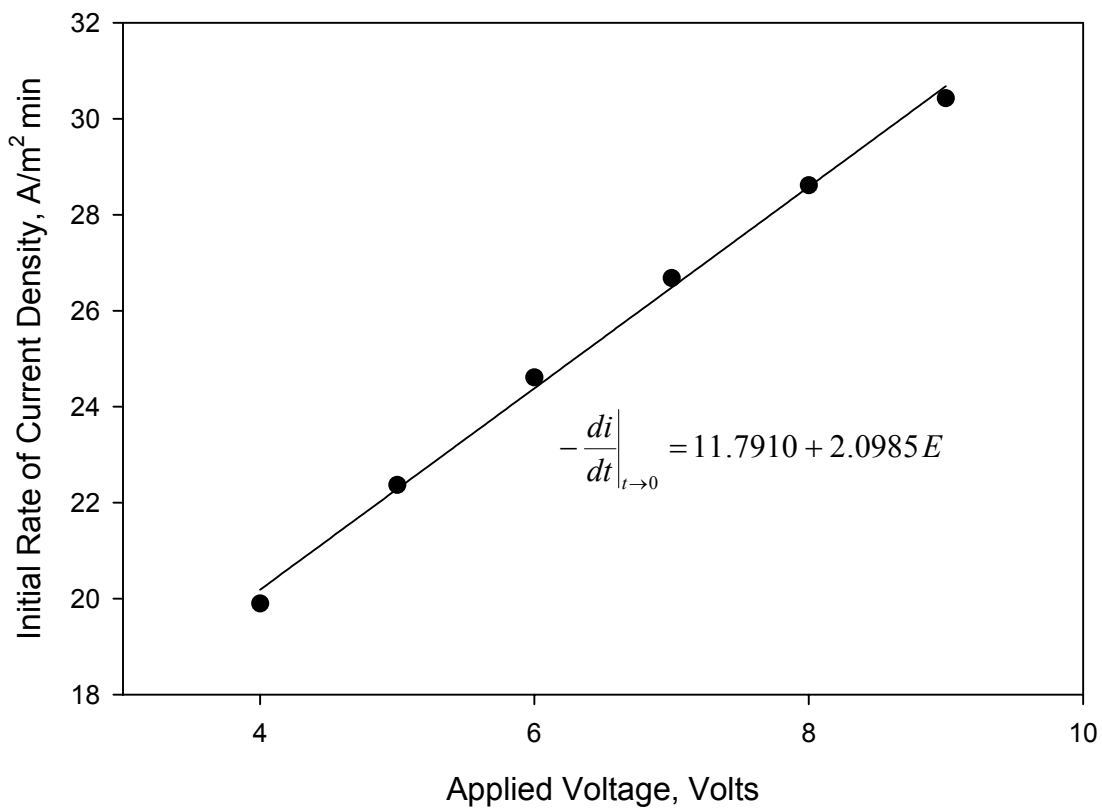


Figure 7. Initial rate of current density as function of the constant applied voltage.

4.3 Electrical Conductivity of Concentrate and Dilute Streams

Figure 8 shows the changes on the electrical conductivity of wheat leachate as a function of time at six constant applied voltages. The electrical conductivity of wheat leachate decreased exponentially with time. The decrease in electrical conductivity was mainly due to the continuous demineralization of wheat leachate. It is observed that there is a significant difference between the electrical conductivity of wheat leachate when operating the cell at applied voltages. A slower decay rate of the electrical conductivity was obtained at 4 volts. Table 6 shows the final electrical conductivity, the initial rate of electrical conductivity from wheat leachate and average standard deviation of data at applied voltages. Figure 9 shows the initial rate of electrical conductivity as a function of the applied voltage. It is observed that the rate increase proportionally with the applied voltage. The initial electrical conductivity rate was correlated as a linear function of voltage:

$$-\left. \frac{dk}{dt} \right|_{\rightarrow 0} = 0.007671 + 0.01743E$$

Where

$$\left. \frac{dk}{dt} \right|_{\rightarrow 0} = \text{Initial electrical conductivity rate, [mS/cm min]}$$

$$E = \text{Applied voltages, [V]}$$

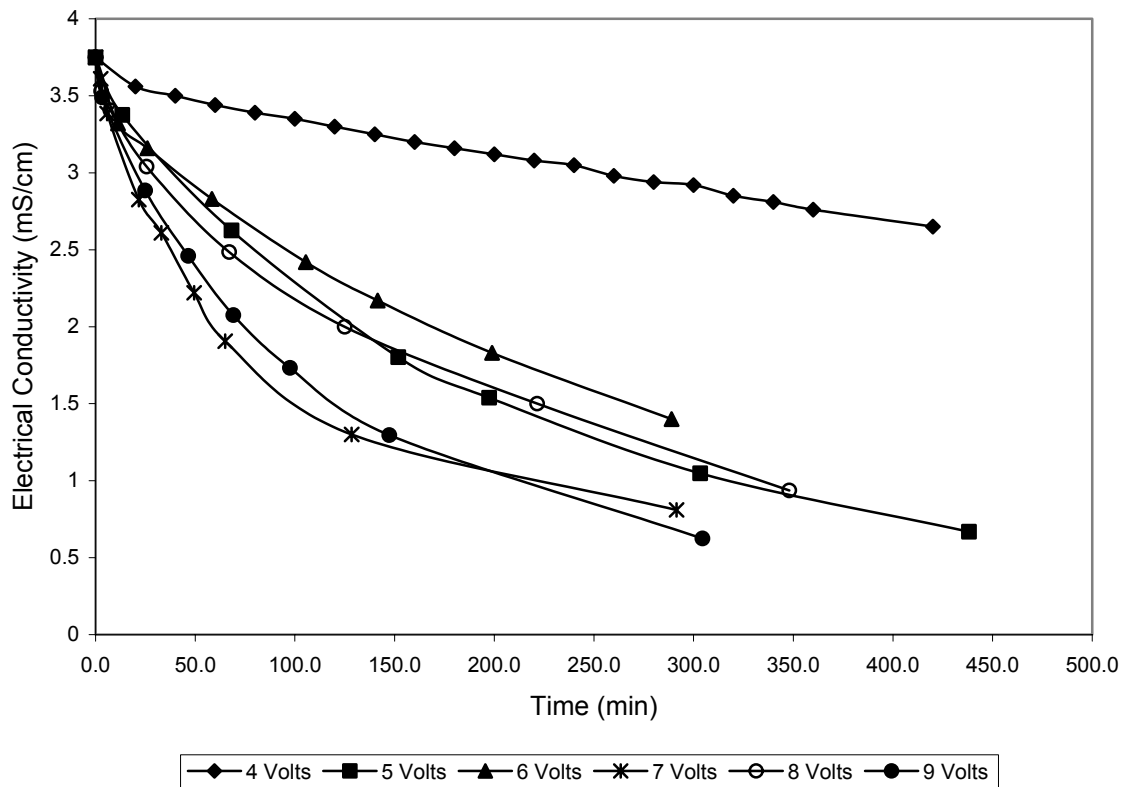


Figure 8. Electrical conductivity for wheat leachate as function of time at constant applied voltage

Table 6. Final electrical conductivity and initial rate of electrical conductivity for applied voltages

Voltages	Final k (mS/cm)	$-\frac{dk}{dt}\Big _{t \rightarrow 0}$	Std. Error.
4	2.65	0.0771	0.0227
5	0.67	0.0949	0.0333
6	1.40	0.1124	0.0202
7	0.81	0.1298	0.0446
8	0.94	0.1476	0.035
9	0.62	0.1640	0.023

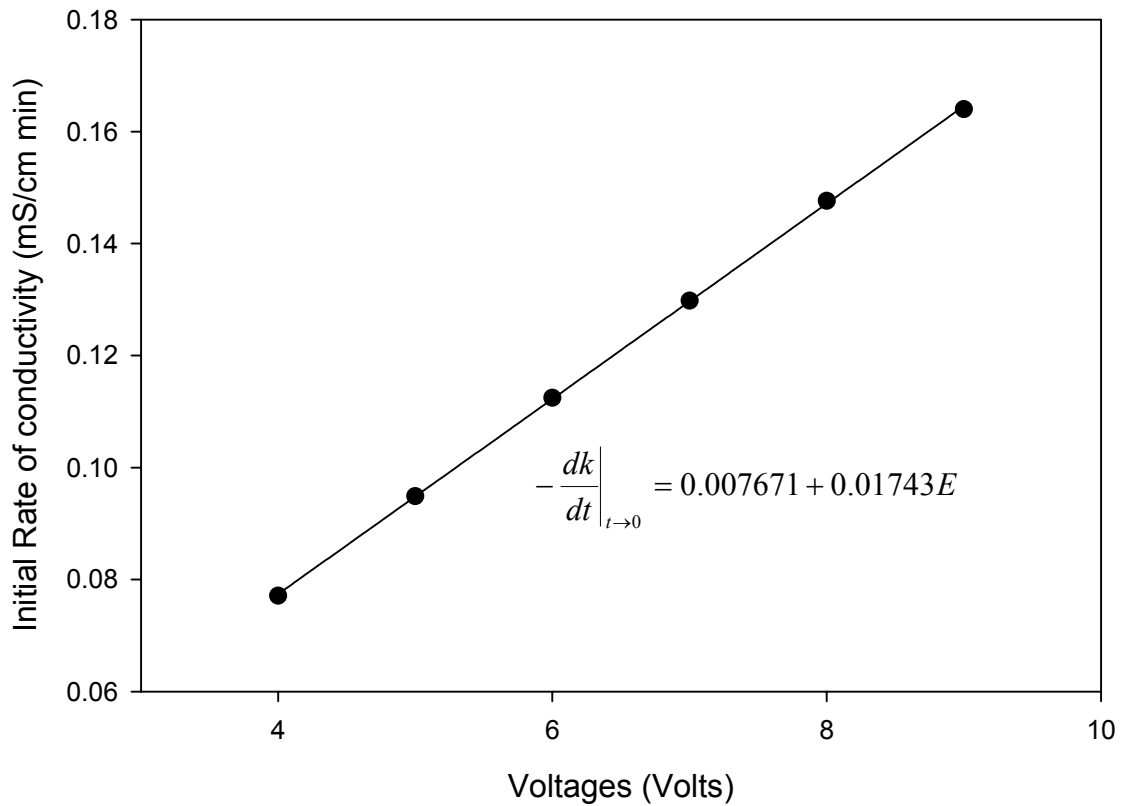


Figure 9. Initial rate of electrical conductivity from wheat leachate as function of applied voltages

Figure 10 shows the electrical conductivity of nitric acid as a function of time. As it can be observed, the electrical conductivity increased rationally with time. There is not a significant difference between the displayed electrical conductivities under the applied voltages. Figure 11 shows the initial electrical conductivity rate of nitric acid. This rate increases proportionally with applied voltages:

$$\left. \frac{dk}{dt} \right|_{t \rightarrow 0} = -0.1119 + 0.0343E$$

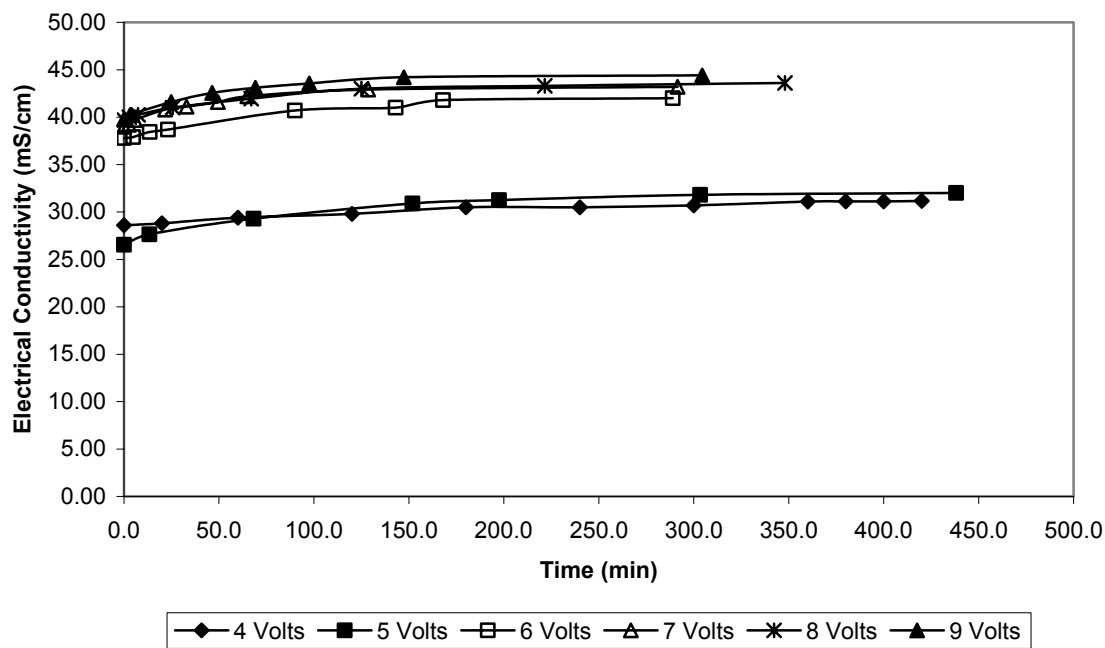


Figure 10. Electrical conductivity of nitric acid at applied voltages

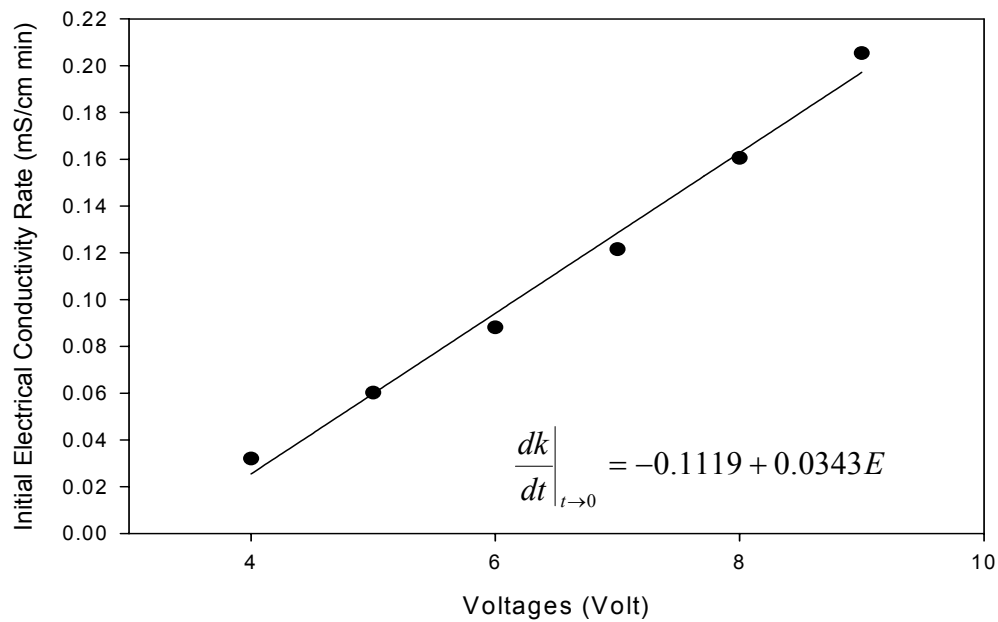


Figure 11. Initial electrical conductivity rate from nitric acid as function of the applied voltage.

4.4 pH of Concentrate and Dilute Streams

Figure 12 shows the changes of pH from wheat leachate as a function of time. As can be observed, there is a not significant difference between the applied voltages. The pH decreases lineally with the time, possibly due to some dissociation of water molecules and other organics present in wheat leachate and directly, due to demineralization of wheat leachate and liberation of hydrogen ions. Table 7 shows the initial and final pH from wheat leachate and average standard deviation of data at applied voltages. At 9 volts the pH concentrate stream decreased more significantly that others applied voltages, as shown the figure 13.

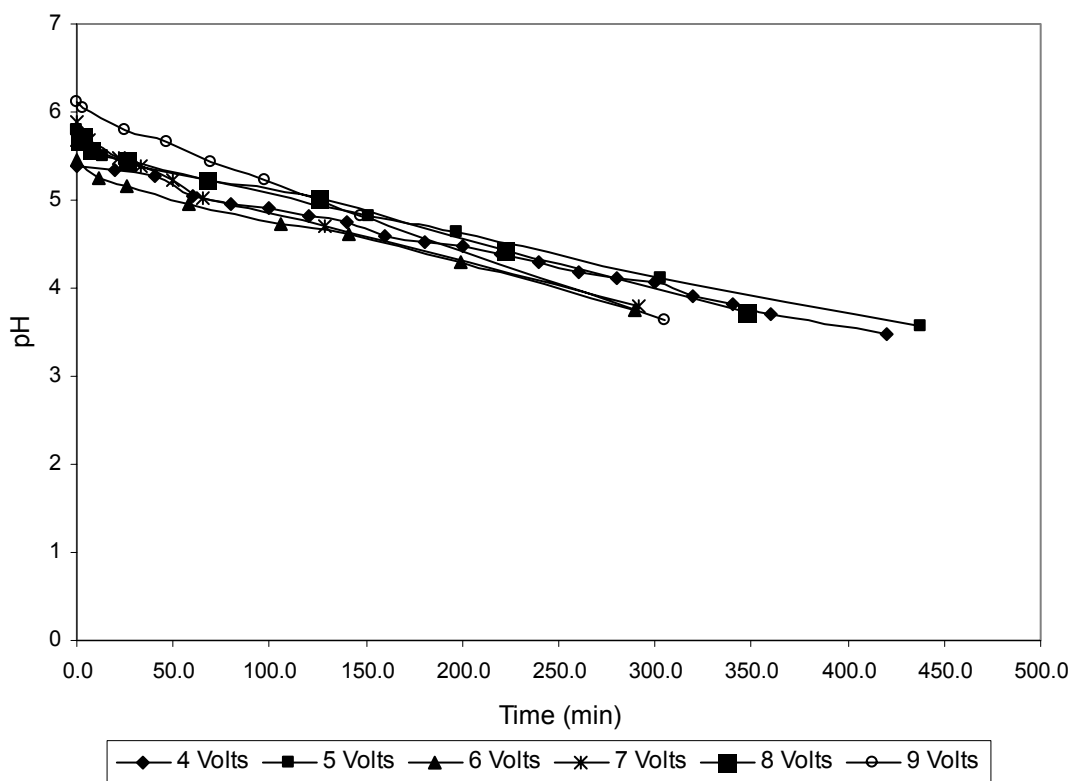


Figure 12. pH versus time of wheat leachate at constant applied voltages.

Table 7. Initial and final pH of wheat leachate

Voltages	Initial pH	Final pH	Std. Error.
4	5.38	3.48	0.1543
5	5.80	3.57	0.0991
6	5.45	3.75	0.0612
7	5.89	3.81	0.1656
8	5.69	3.72	0.0521
9	6.12	3.64	0.0558

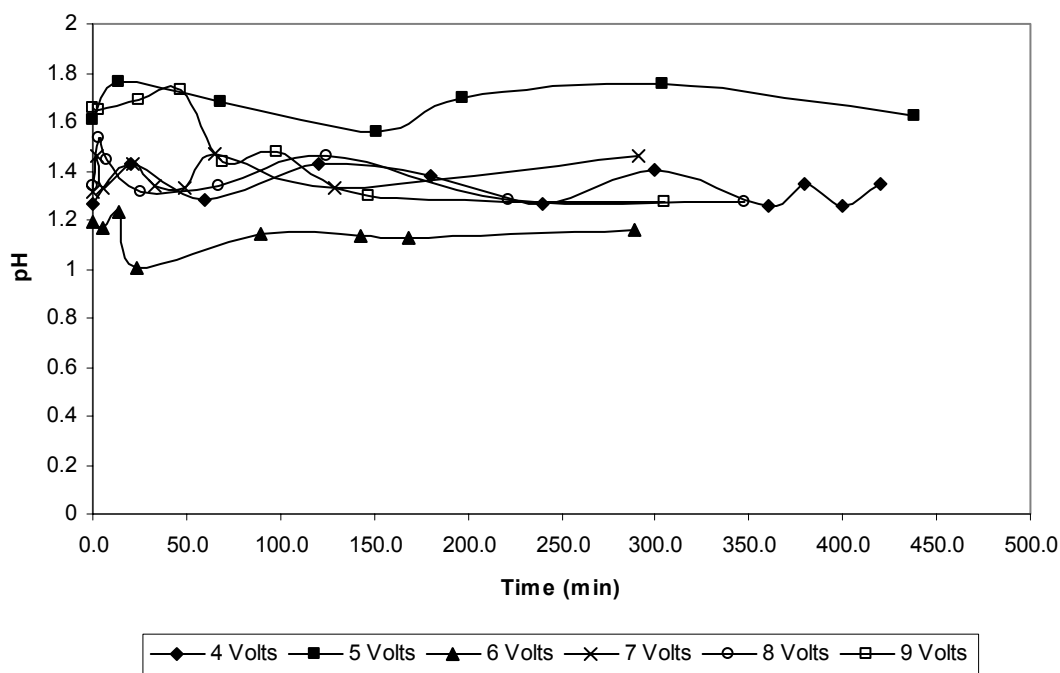


Figure 13. pH of nitric acid at different constant applied voltages.

4.5 Total Organic Carbon

The total organic carbon (TOC) of wheat leachate as a function of time and applied voltage is shown in Figure 14. The TOC decreases with time and applied voltages. At constant voltages, the organic molecules are ionized, transferred through the membrane causing internal blocking. Most of the organics present in

wheat leachate had a negative charge, these organic anions are attracted to anion membrane when a voltage field is applied, this explains because the anion-exchange membrane has more fouling than the cation-exchange membrane. Figure 14 shows that for lower voltages, the TOC decrease slighter than for higher voltages. At higher voltages, there is more energy to ionize the organic molecules and this reduces, more significantly, TOC in wheat leachate with the time. Figure 15 shows initial TOC rate at constant applied voltages. The initial TOC rate increase proportionally with applied voltage. This behavior was correlated as a linear function of voltage:

$$-\left. \frac{dTOC}{dt} \right|_{t \rightarrow 0} = -13.6292 + 10.9711E$$

Where,

$$\left. \frac{dTOC}{dt} \right|_{t \rightarrow 0} = \text{Initial TOC Rate}$$

Table 8 shows the decrease in the TOC from wheat leachate and initial TOC rate at applied voltages. Though TOC decreases directly with applied voltage, there is not significant difference in the final TOC and total decrease percentage at 7 and 8 Volts and 6 and 9 Volts, respectively, as shown Table 8 and Figure 14.

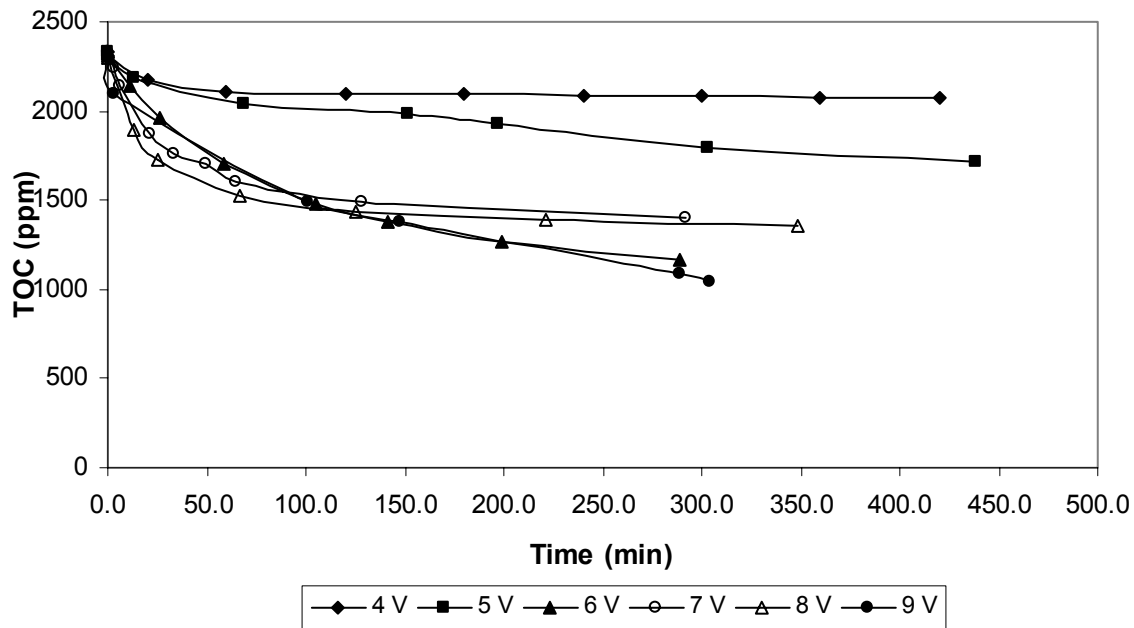


Figure 14. TOC of wheat leachate as function of time at constant applied voltage.

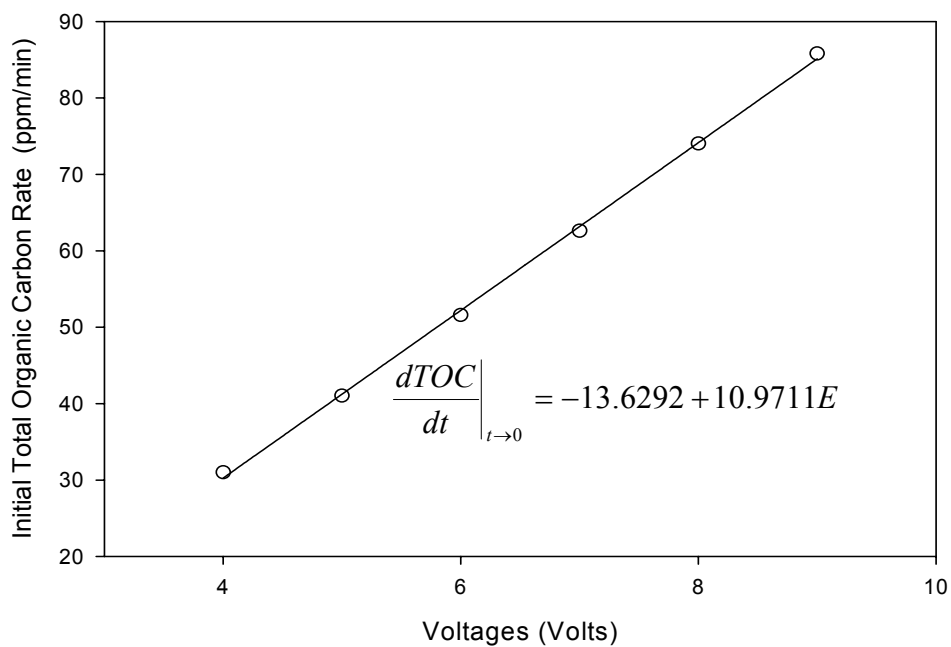


Figure 15. Initial TOC rate as function of the applied voltage.

Table 8. Decrease of TOC and initial TOC rate at applied voltage.

Voltage (Volts)	$-\left.\frac{dTOC}{dt}\right _{t \rightarrow 0}$	Final TOC	Decrease TOC (%)
4	31.0158	2074.39	10.99
5	41.0398	1712.92	26.50
6	51.5914	1169.92	49.80
7	62.6046	1402.29	39.83
8	74.0240	1361.93	41.56
9	85.8200	1043.78	55.21

4.6 Removal of Ions from Dilute Stream

Figure 16 shows the percent nitrate removal from wheat leachate as function of time. At 4 Volts, the removal of nitrate is 44 %, the lowest. At low current densities, as result of low voltages, the flow of ions is lower than at high voltages. Moreover, it is observed back diffusion before 100 minute at this voltage, as consequence of saturation in the active places of anion membrane, this phenomenon is explain in the section 4.8. The removal of nitrate is over 96 % at 5 to 9 Volts. Table 9 shows the nitrate removal and initial nitrate removal rate at constant applied voltages. The initial nitrate removal rate as function of applied voltage increases proportionally (Figure 17). The function applied to this relation is a power function:

$$\left.\frac{dR_{NO_3}}{dt}\right|_{t \rightarrow 0} = 0.0757 E^{2.3151}$$

Where,

$$\left.\frac{dR}{dt}\right|_{t \rightarrow 0} = \text{Initial nitrate removal rate, [\%/min]}$$

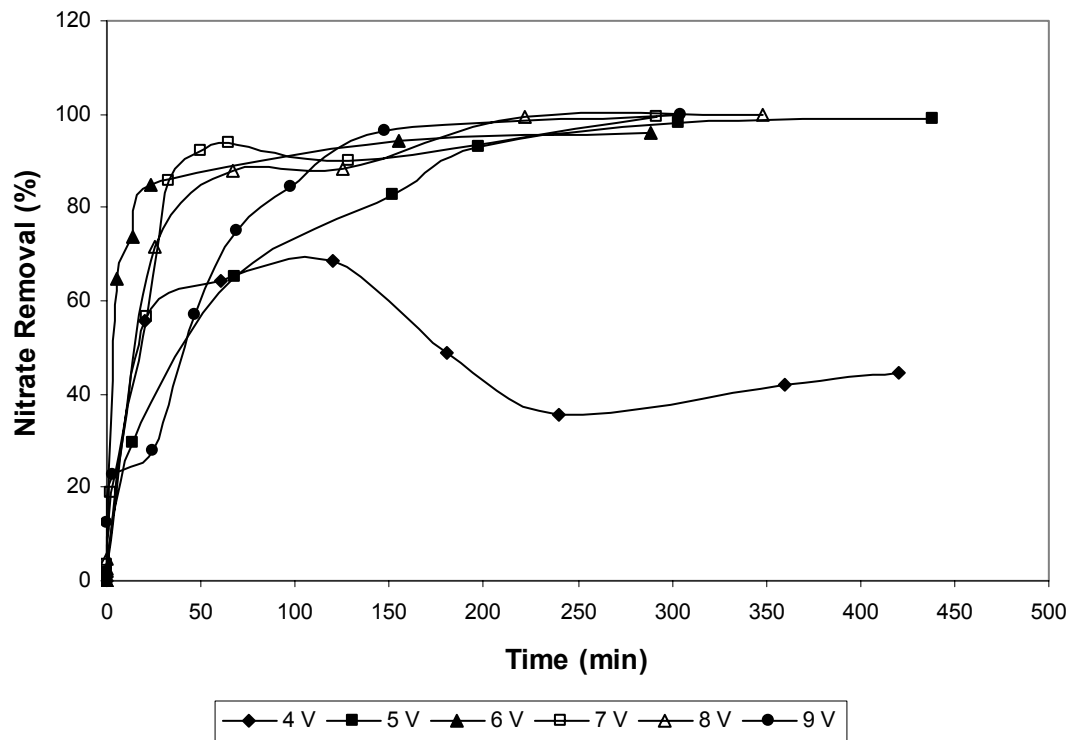


Figure 16. Nitrate removal from wheat leachate as function of time at constant applied voltage.

Table 9. Nitrate removal and initial nitrate removal rate at constant applied voltages

Voltages (Volts)	Nitrate removal (%)	Initial nitrate removal rate (%/min)
4	44.44	1.8756
5	99.07	3.1442
6	96.12	4.7956
7	99.25	6.8520
8	99.71	9.3347
9	100.00	12.2604

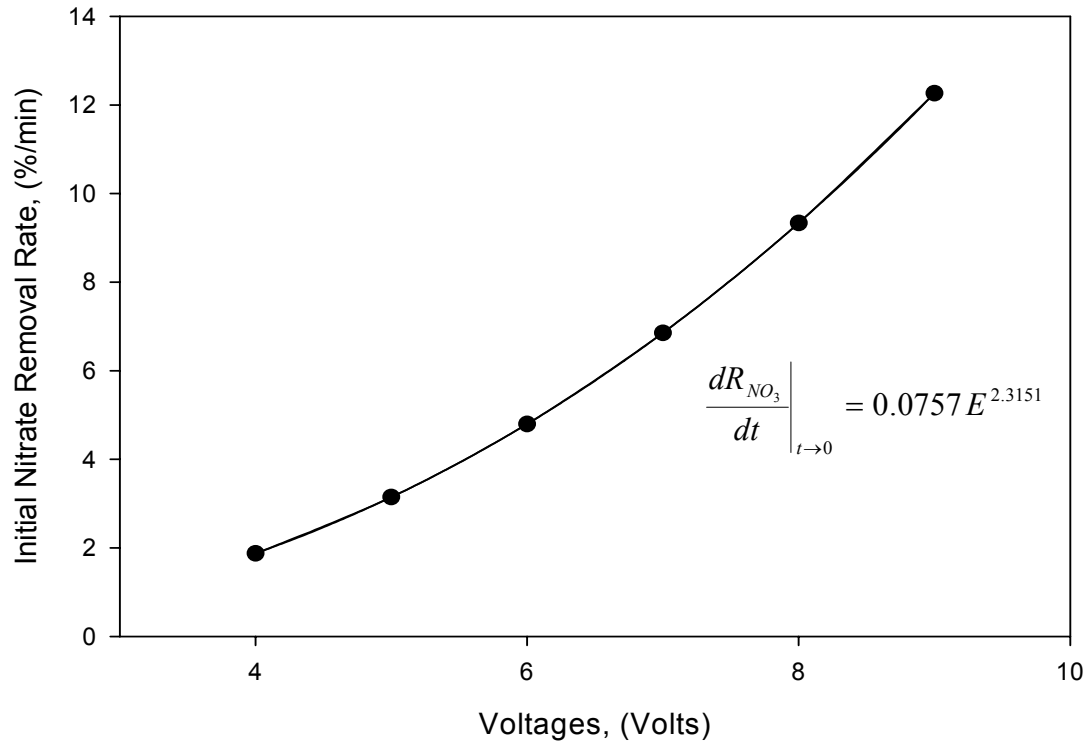


Figure 17. Initial rate of nitrate removal as function of the applied voltage.

Potassium percent removal as function of the time is showed in the Figure 18. Table 10 shows the maximum potassium removal and initial potassium removal rate at constant voltage. The potassium removal is between 97 to 99 % for 5, 6, 7, 8 and 9 Volts. The lower potassium removal is 63.27 % at 4 Volts. The initial potassium removal rate increases with applied voltage, see Figure 19. The function that predicted this behavior is a power function:

$$\frac{dR_k}{dt} \Big|_{t \rightarrow 0} = 0.0354 E^{2.254}$$

Where,

$$\left. \frac{dR_k}{dt} \right|_{t \rightarrow 0} = \text{Initial potassium removal rate, [\%/min]}$$

Figure 20 shows the removal of anions from leachate for batch operation mode at 4, 5, 6, 7, 8 and 9 volts. The removal of anions increased with time. As it's observed in the Figure 20, the percent removal of nitrate and chloride, monovalent anions, is the highest, this suggest that, the anion-selective membrane used in this study was more efficient in the removal of monovalent anions (NO_3^- and Cl^-) than for divalent anion and trivalent anion (SO_4^{2-} and PO_4^{3-} , respectively). The removal of the fluoride anion is the lowest, as shown Figure 20. After 100 min, there is back diffusion at 4 volts due to membrane fouling. At this voltage, the active places of membrane are taken by organic anions and the membrane selectivity decreases as result of a poor mobility of organic anions at low voltages. Moreover, Figure 21 shows that the initial rate of nitrate concentration increases with applied voltages. The initial rate of nitrate concentration, at the applied voltages, is shown in Table 11. The initial nitrate concentration rate was correlated as a power function of voltage:

$$-\left. \frac{dC}{dt} \right|_{t \rightarrow 0} = 170.2923E^{0.3216}$$

Where:

$$\left. \frac{dC}{dt} \right|_{t \rightarrow 0} = \text{Initial nitrate concentration rate, [ppm/min]}$$

Figure 22 shows percent removal of cations from leachate as a function of time at different constant applied voltages. The final removal of cations is the same at different constant applied voltages, this proposes that, the used cation-exchange membrane is not significantly different in the selectivity for monovalent cation (potassium) and bivalent cations (magnesium and calcium). At 4 volts, there is no back diffusion due to the absence of fouling on the cation membrane.

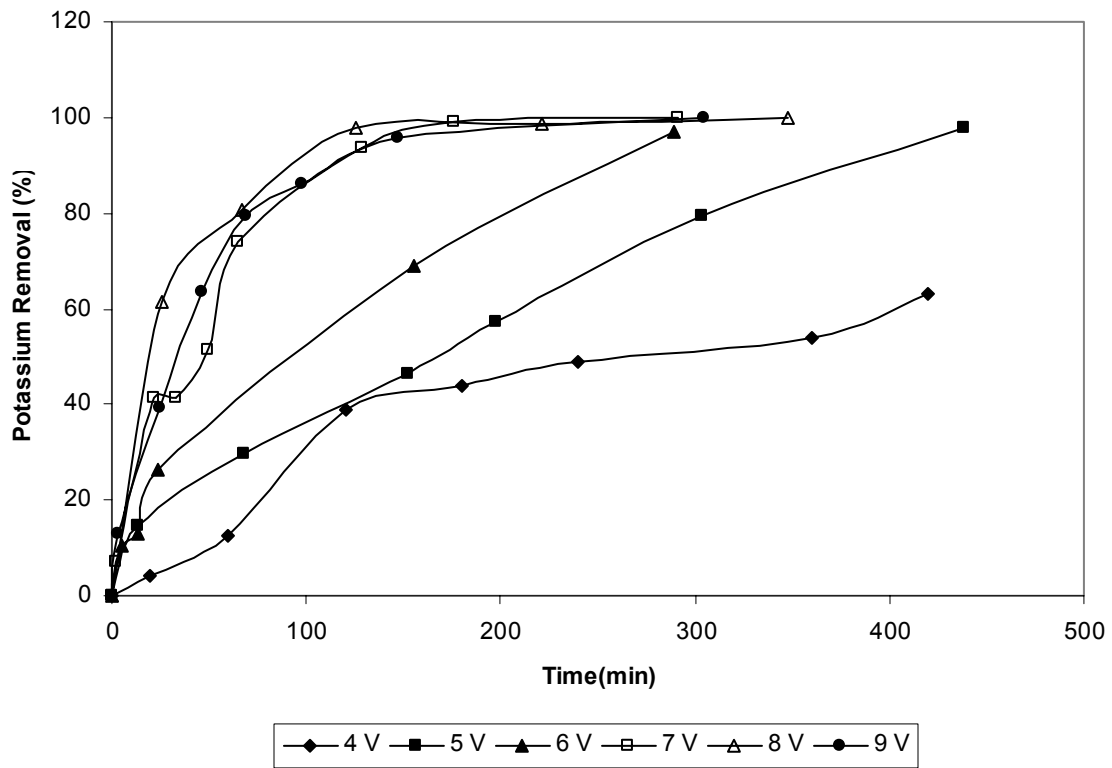


Figure 18. Potassium removal from wheat leachate as function of the time at constant applied voltage.

Table 10. Potassium removal and initial potassium removal rate at constant applied voltages

Voltages (Volts)	Potassium removal (%)	Initial potassium removal rate (%/min)
4	63.2674149	0.8055
5	97.6465962	1.3321
6	97.1383805	2.0090
7	99.2828695	2.8440
8	97.7472738	3.8429
9	99.8199348	5.0110

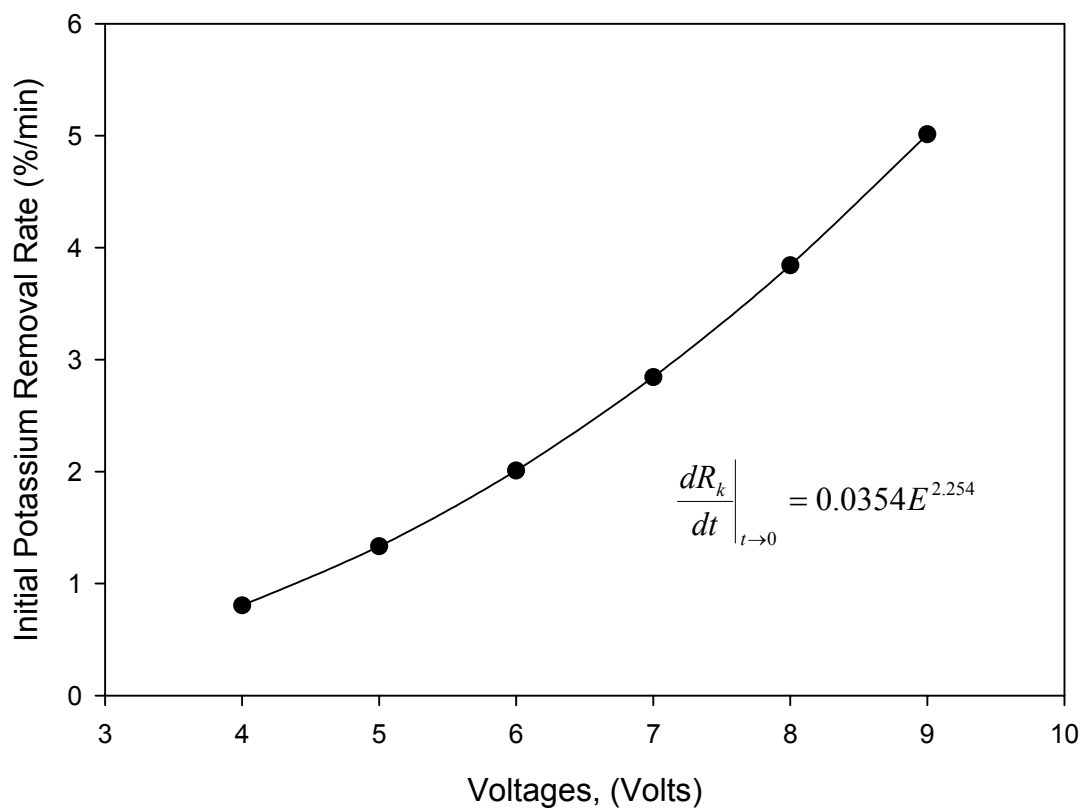


Figure 19. Initial rate of potassium removal as a function of the applied voltage.

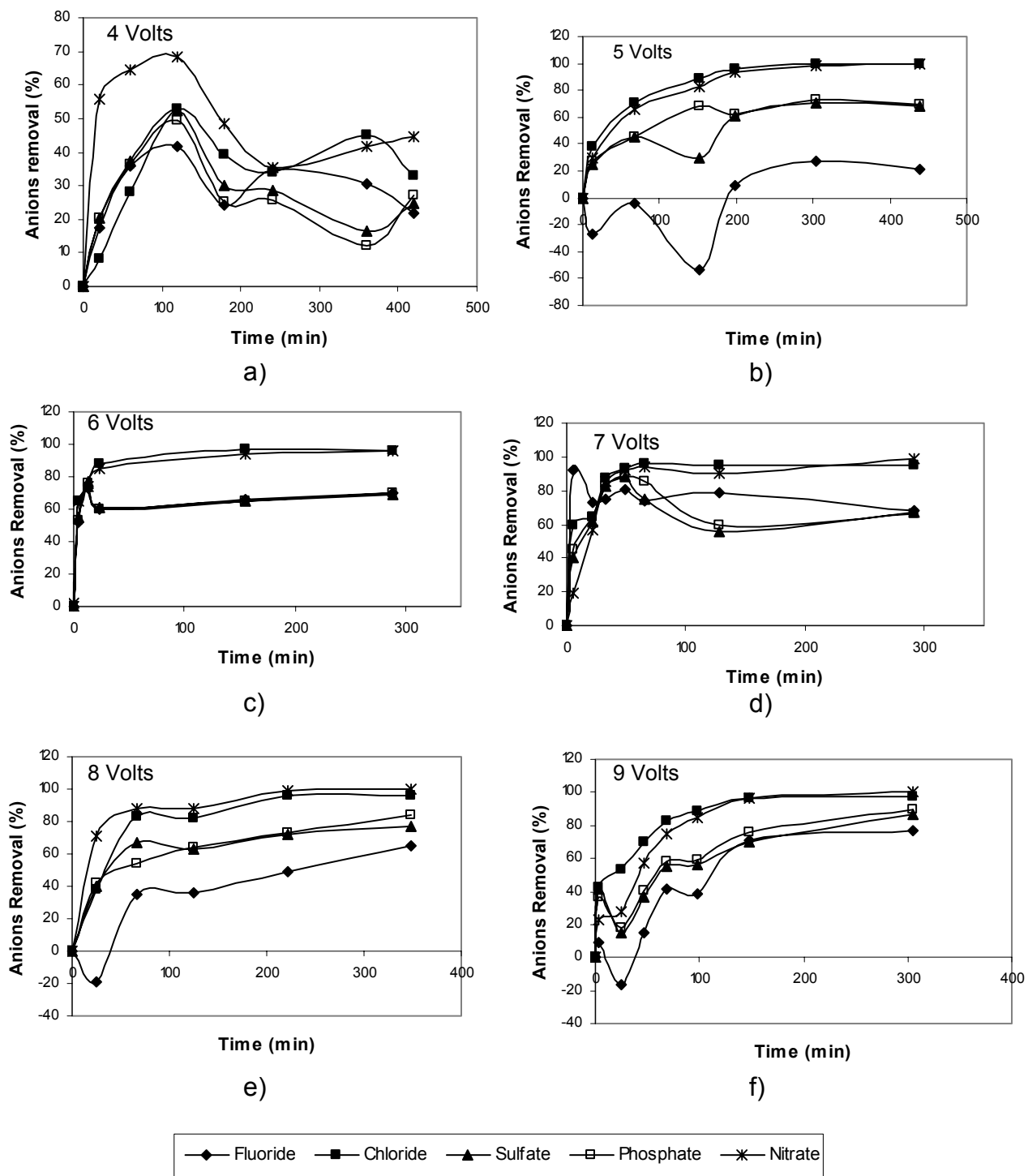


Figure 20. Anions Removals as a function of time at constant applied voltages. a) 4 Volts, b) 5 Volts, c) 6 Volts, d) 7 Volts, e) 8 Volts, f) 9 Volts.

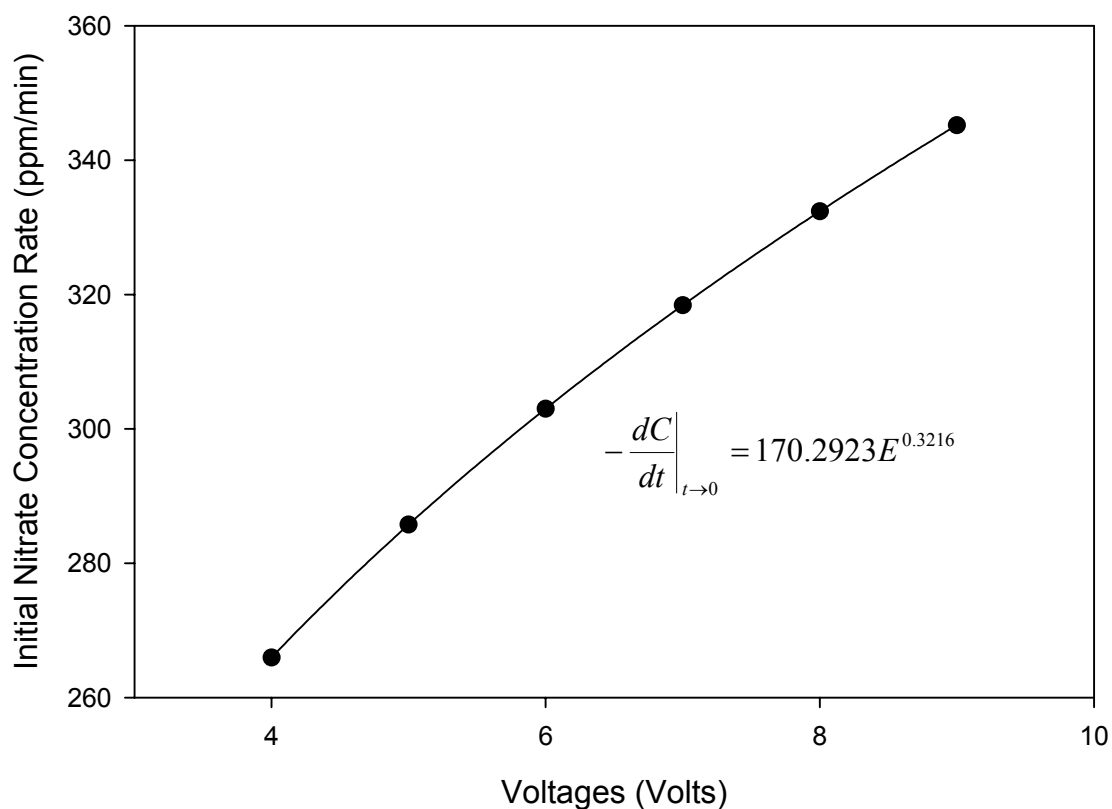


Figure 21. Initial Rate of Nitrate Concentration as a function of applied voltage.

Table 11. Initial rate of nitrate concentration at applied voltages

Voltages (Volts)	Initial rate of nitrate concentration (ppm/min)
4	265.9547
5	285.7419
6	303.0000
7	318.4000
8	332.3600
9	345.1991

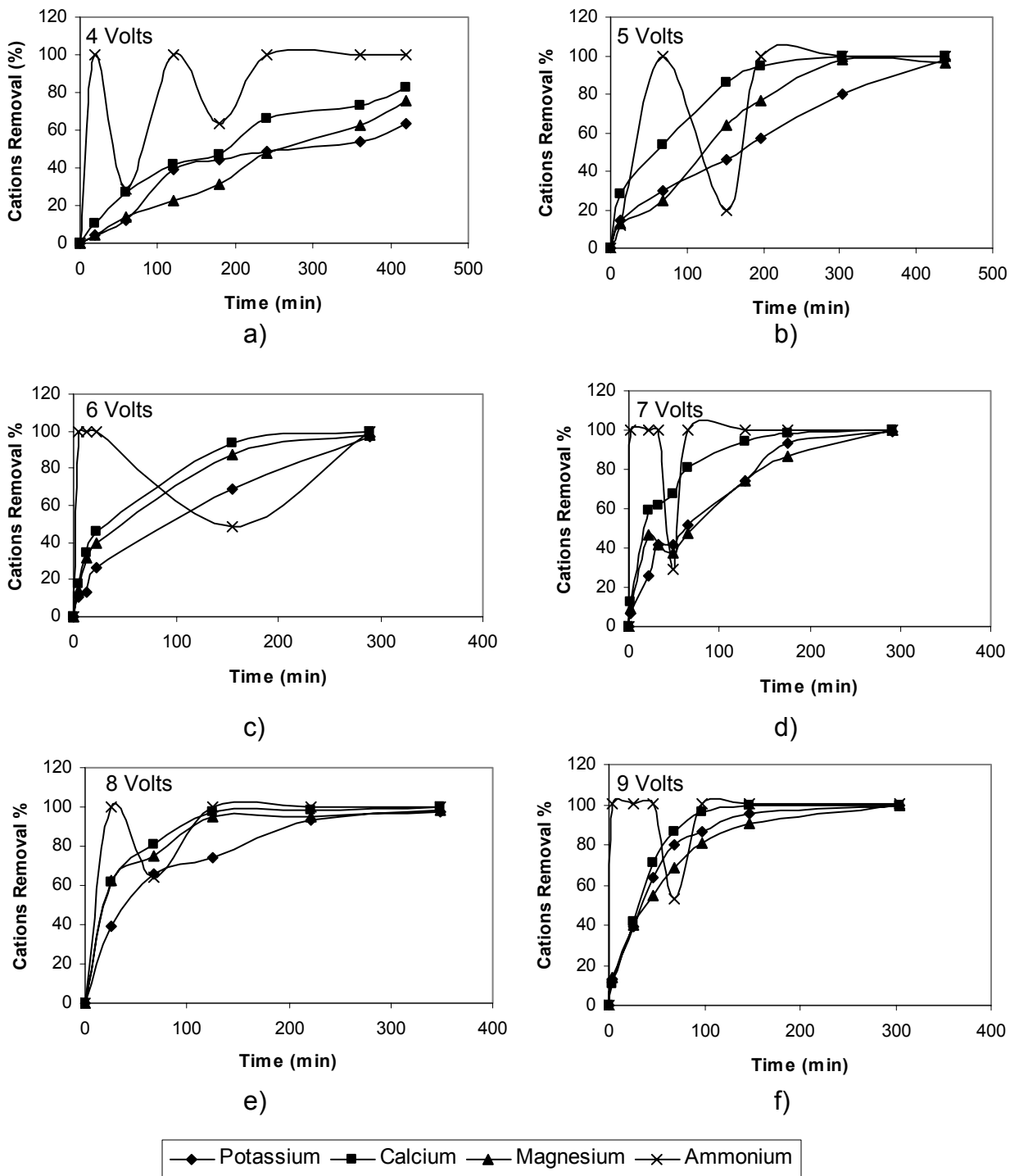


Figure 22. Cations Removals as a function of time at constant applied voltages. a) 4 Volts, b) 5 Volts, c) 6 Volts, d) 7 Volts, e) 8 Volts, f) 9 Volts.

4.7 Anions at Nitric Acid Solution

Figures 23 and 24 show the anions chart for 5 and 9 volts from nitric acid, respectively. As can be observed, the anions concentration increase with the time at applied voltage. The concentration increase is proportional to the expected raise of removal percentage from wheat leachate.

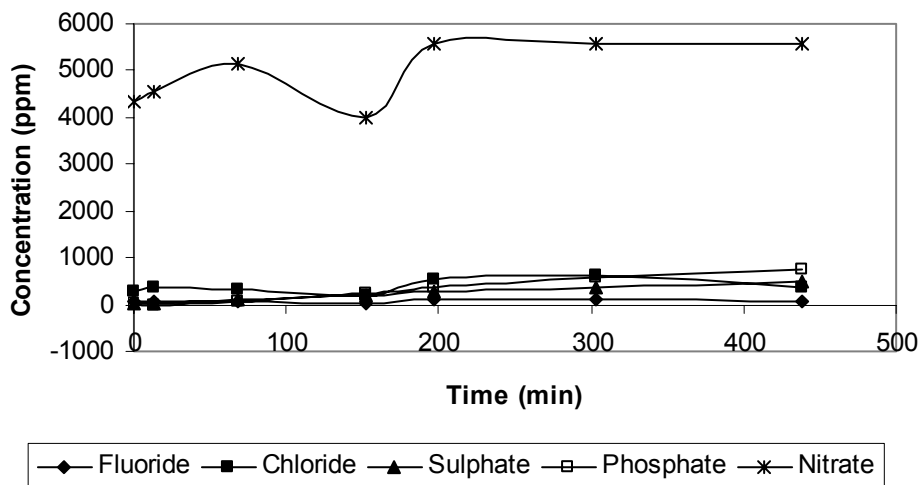


Figure 23. Anions Chart from nitric acid at 5 volts

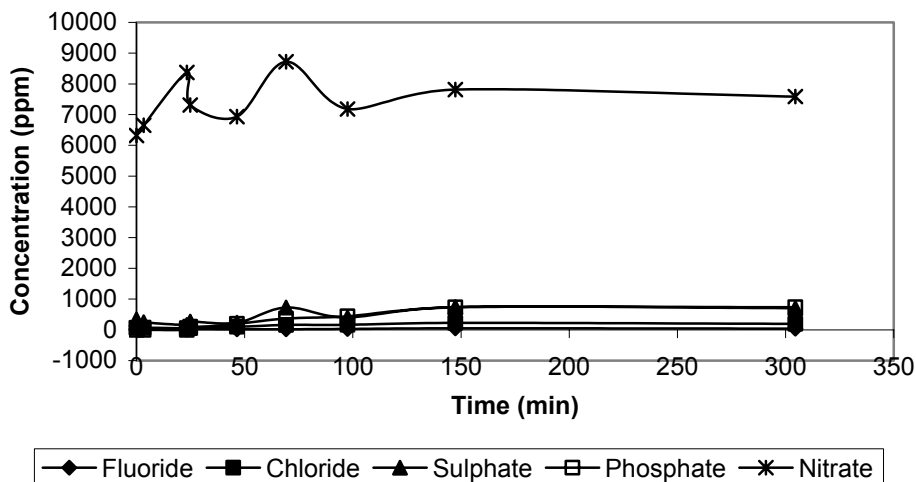


Figure 24. Anions Chart from nitric acid at 9 volts

4.8 Fouling Results

Figure 25 shows the electrical resistance of the anion-exchange membrane and wheat leachate solution as a function of time. The initial measurement of electrical resistance corresponds to the initial electrical resistance of anion membrane without the initial electrical resistance of fluid. The electrical resistance of the system, fluid and anion membrane, increase with time. At 100 mV, the electrical resistance increase is lower than at 75mV and 25 mV, maybe due to effects of the voltage over the wheat leachate solution. The increase in the membrane electrical resistance, as indicator of membrane fouling, takes place when the flow paths for the ions are restricted. In some way, the fluid electrical resistance increase is due conductivity decrease from wheat leachate solution, as result of ions decrease. As shows in Table 12, the final membrane electrical resistance decreases with applied voltage. Moreover, it can be observed that the initial fluid electrical resistance changes with applied voltages. The final electrical resistance of anion membrane decreases with applied voltage possible due to a higher ions mobility in the membrane at high voltages. The decrease of fouling on anion membrane, at high voltages, can be due to higher anion organic molecules of the wheat leachate through the anion membrane. At low voltages, the anion organic molecules reach the anion membrane surface but the electromotive force is not sufficiently high so that this molecules can go through the anion membrane. This occurs because the Van der Waals interactions between these molecules and the active groups of anion membrane are stronger than the electromotive force. Before the beginning of the experiments, and without applied voltage, it was observed that the fluid electrical resistance decrease with the time, it isn't constant. But, during the experiments, at constant voltage, the fluid electrical resistance increases with the time as shown Figure 25. In this Figure, the final electrical resistance of the system, at constant applied voltages, is higher than the shown results of final electrical resistance of membrane, in Table 12, this as compensation of the fluid electrical resistance increase. The fluid electrical resistance is inversely proportional of

electrical conductivity and concentration of ions from solution, this suggests that without applied voltage the ion organic molecules form agglomerates that precipitate in the solution, this phenomenon facilitate the pass the current through of the wheat solution, as result the electrical resistance decreases.

Figure 26 shows the electrical resistance of the cation-exchange membrane and wheat leachate solution as a function of the time at constant applied voltage. The initial measurement of electrical resistance corresponds to the initial electrical resistance of the complete system. As can be observed, the electrical resistance change of the system is not significant at 25 mV and 50 mV due the poor concentration of cation organic molecules. At high voltages, 75 mV and 100 mV, the electrical resistance, or fouling, increases as result of high mobility of organic molecules by electromotive force of applied field (see Figure 26 and Table 13). The fluid electrical resistance changes during those experiments are smaller than the changes of fluid electrical resistance at anion-exchange membrane. This behavior may be due to the low concentration of cation organic molecules and the decrease of ions transfer.

Table 12. Final electrical resistance of anion membrane and initial fluid electrical resistance.

Voltage (mV)	Operation time (min)	Final membrane electrical resistance (Ohm cm ²)	Initial fluid electrical resistance (Ohm-cm ²)	Fluid Resistivity (Ohm-cm)
0	1310	232.12	250.31	37.54
25	70	437.46	250.31	37.54
50	45	374.97	277.79	41.67
75	100	312.47	219.78	32.97
100	175	278.38	67.81	10.17

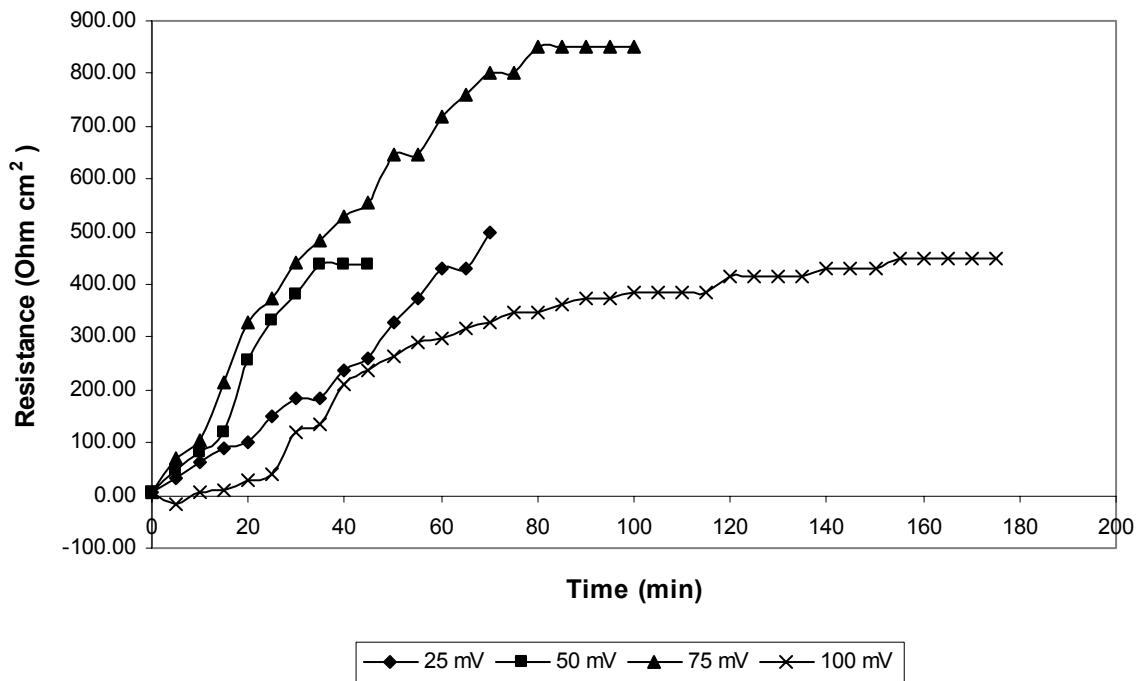


Figure 25. Electrical resistance of the anion-exchange membrane and wheat leachate solution as a function of the time at applied voltages.

Table 13. Final electrical resistance of cation membrane and initial fluid electrical resistance.

Voltage (mV)	Operation time (min)	Final membrane electrical resistance (Ohm cm ²)	Initial fluid electrical resistance (Ohm-cm ²)	Fluid Resistivity (Ohm-cm)
0	0	10.6992935	266.2290677	39.93
25	70	10.6992935	266.2290677	37.54
50	45	10.6992935	292.487296	43.81
75	100	218.731042	349.9271704	52.48
100	175	312.472917	284.0846629	42.61

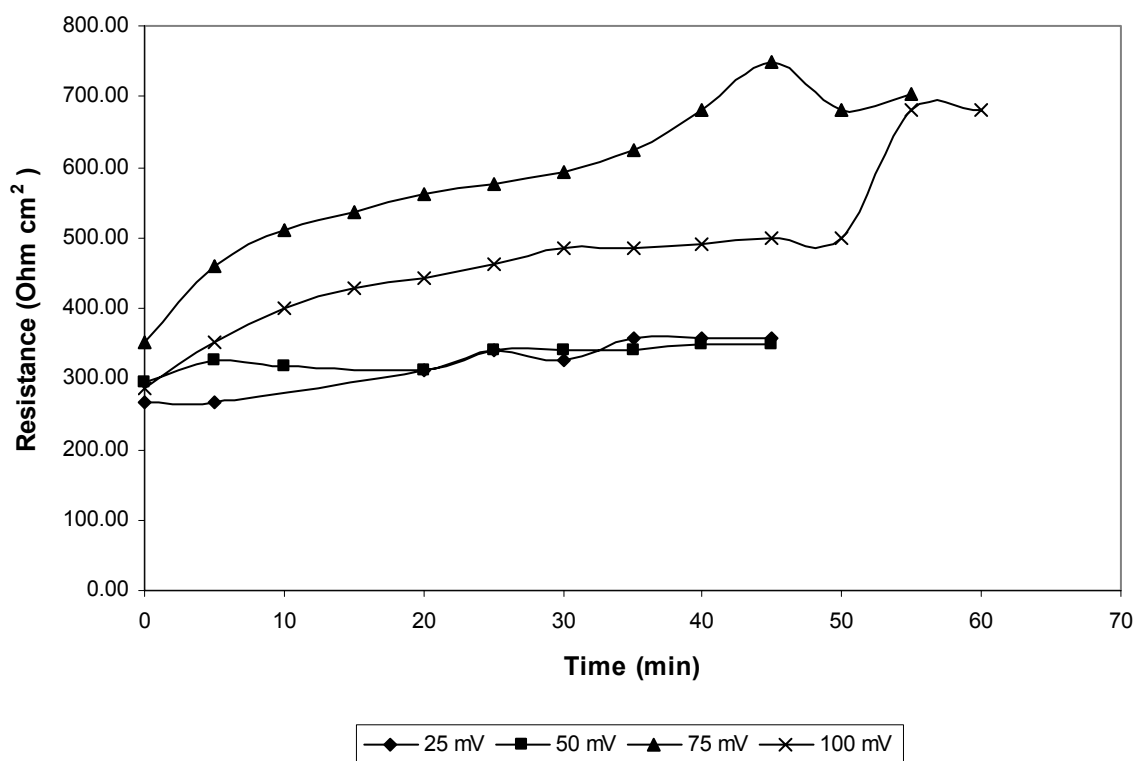


Figure 26. Electrical resistance of the cation-exchange membrane and wheat leachate solution as a function of the time at constant applied voltages.

4.9 Generation of Nitrogen and Oxygen

Figures 27 and 28 show the generation of molecular oxygen (O_2) and molecular hydrogen (H_2), respectively. The oxygen and hydrogen generation are higher at 7 volts and 9 volts, than at other voltages. At 6, 5 and 8 volts, there are no significant differences. The production of gases, at 4 volts, is lower. Table 14 shows the final production of oxygen and hydrogen at applied voltages.

The electrolytic reactions that take place in the cathode compartment and anode compartment are:



When the electrical potential is applied to the electrolytic cell, hydroxide ions are obtained by water electrolysis in the cathode compartment to produce potassium hydroxide. The electrolytic reduction of water also produce hydrogen gas (Figure 28). As is expected at low voltages the generated hydrogen gas is low (Figure 28). The necessary energy to break the covalent bond of water in the reduction reaction is higher than in the oxidation reaction. Maybe, the electrons migration is scattered by diverse forms as heat by conduction. The oxidation of water produce bigger amount of hydrogen ions, as can be seen in the Figure 27 because the necessary energy is lower than reduction reaction.

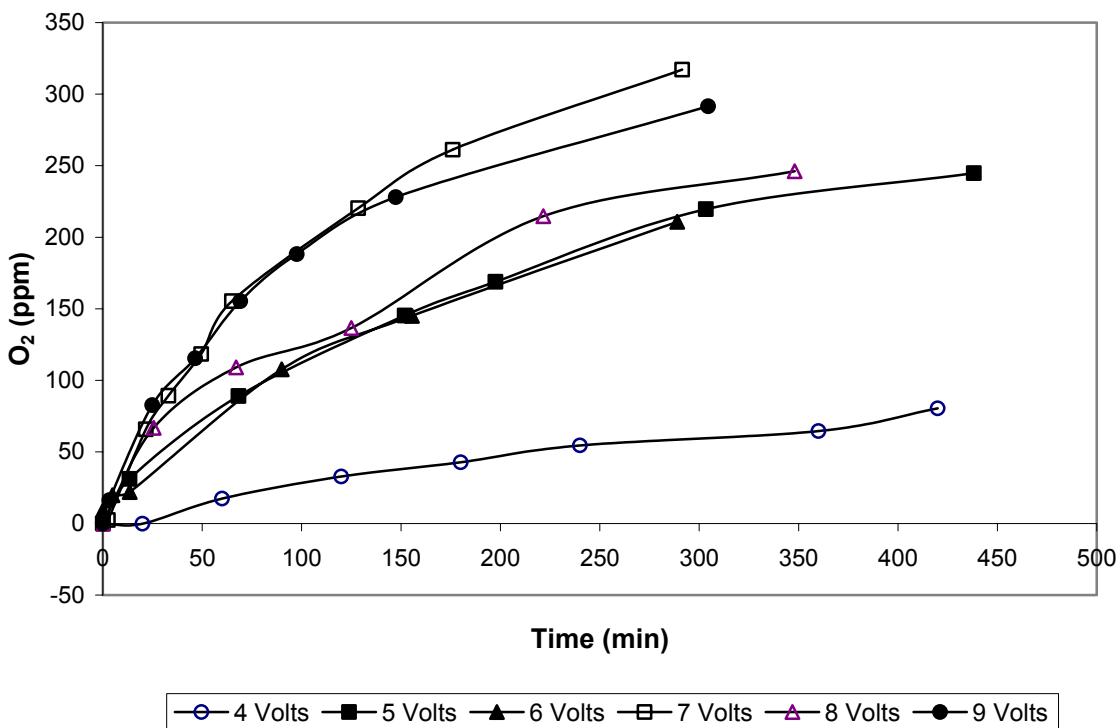


Figure 27. Production of oxygen as a function of time at constant applied voltages

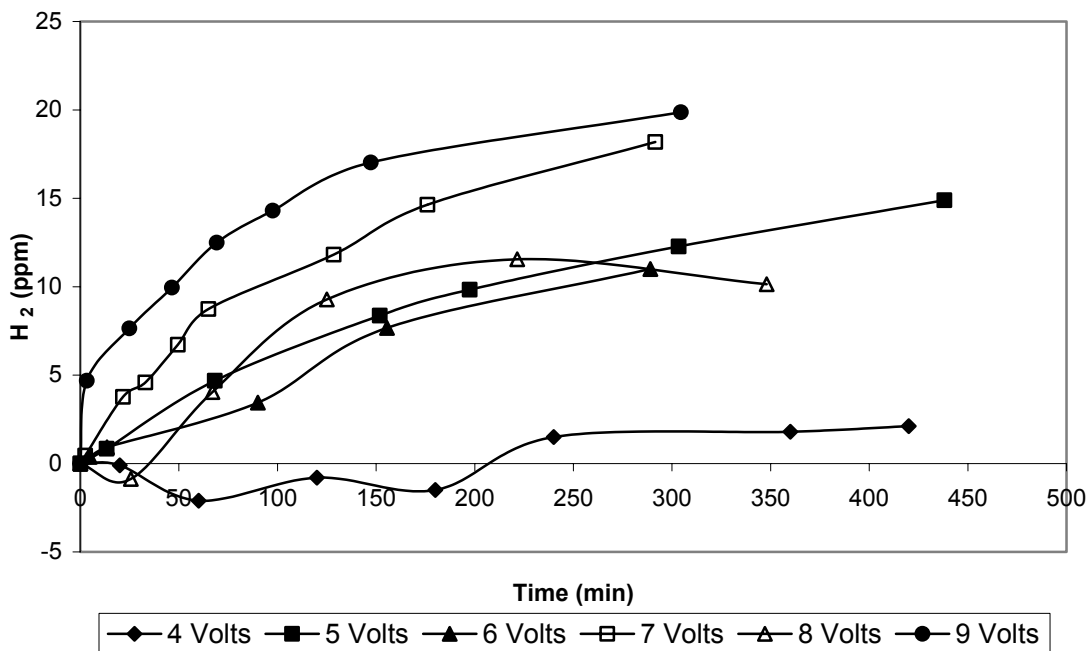


Figure 28. Production of hydrogen as a function of time at constant applied voltage.

Table 14. Final and Total production of oxygen and hydrogen at batch processes.

Voltages (Volts)	O ₂ Final production (ppm)	Total production O ₂ (mg)	H ₂ Final production (ppm)	Total Production H ₂ (mg)
4	80.47	724.22	2.11	18.99
5	244.74	2202.69	14.89	133.99
6	210.84	1897.61	10.99	98.97
7	317.06	2853.52	18.19	163.69
8	246.06	2214.51	10.14	91.24
9	291.48	2623.33	19.87	178.83

4.10 Normality of Nitric Acid

Figure 29 shows the changes of nitric acid concentration as a function of time at constant applied voltage. Normality of the concentrate stream increased logarithmically with time. As can be observed, the normality increases with applied voltage, having the lowest normality increase at 4 volts. Table 15 shows the increase percentage of nitric acid at constant applied voltages. The higher increase is reached at 5 volts, followed by 7 volts. As it is expected, the lower increase is obtained at 4 volts. Figure 30 shows the normality of potassium hydroxide as a function of time. As can be observed, the normality increases with time at constant applied voltage, due the production of hydrogen in the cathode of electrolytic cell. At 4 volts, the normality increase of potassium hydroxide is light. Table 16 shows the increase of potassium hydroxide with applied voltage. At 5, 7 and 9 Volts the increase of normality is higher.

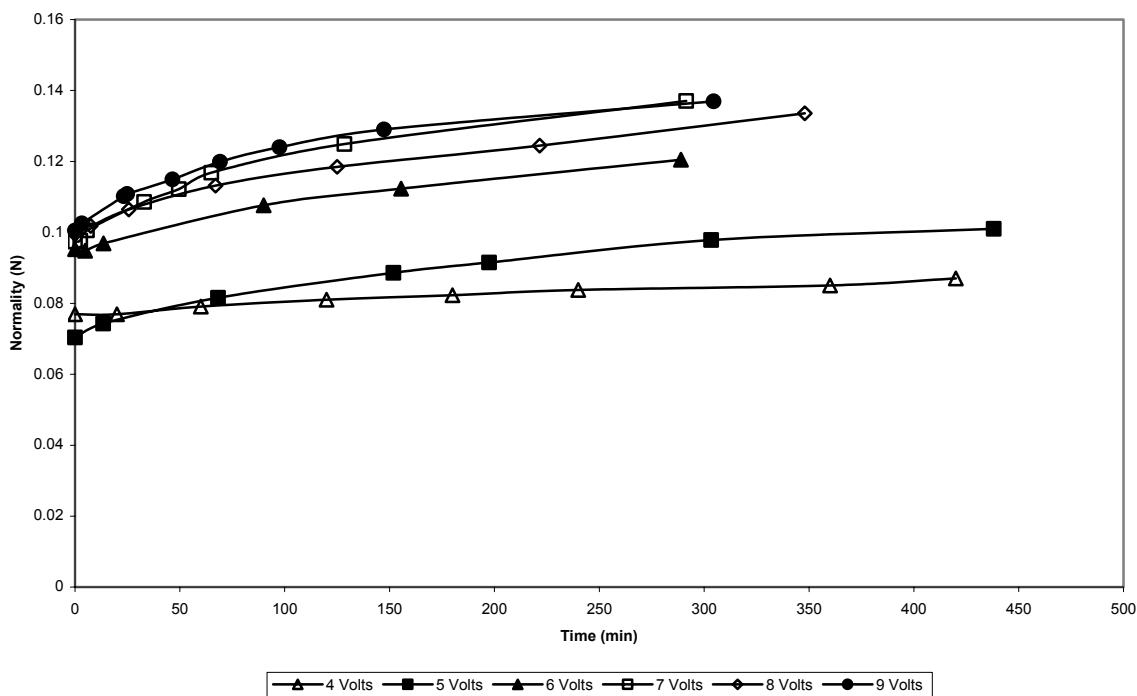


Figure 29. Normality of nitric acid as a function of time at constant applied voltage for batch operation.

Table 15. Normality of nitric acid at constant applied voltage.

Voltages (Volts)	Initial Normality (N)	Final Normality (N)	Increase Percentage (%)
4	0.0769	0.087	13.08
5	0.0704	0.101	43.45
6	0.0953	0.1205	26.48
7	0.0974	0.137	40.69
8	0.0995	0.1336	34.21
9	0.1005	0.137	36.25

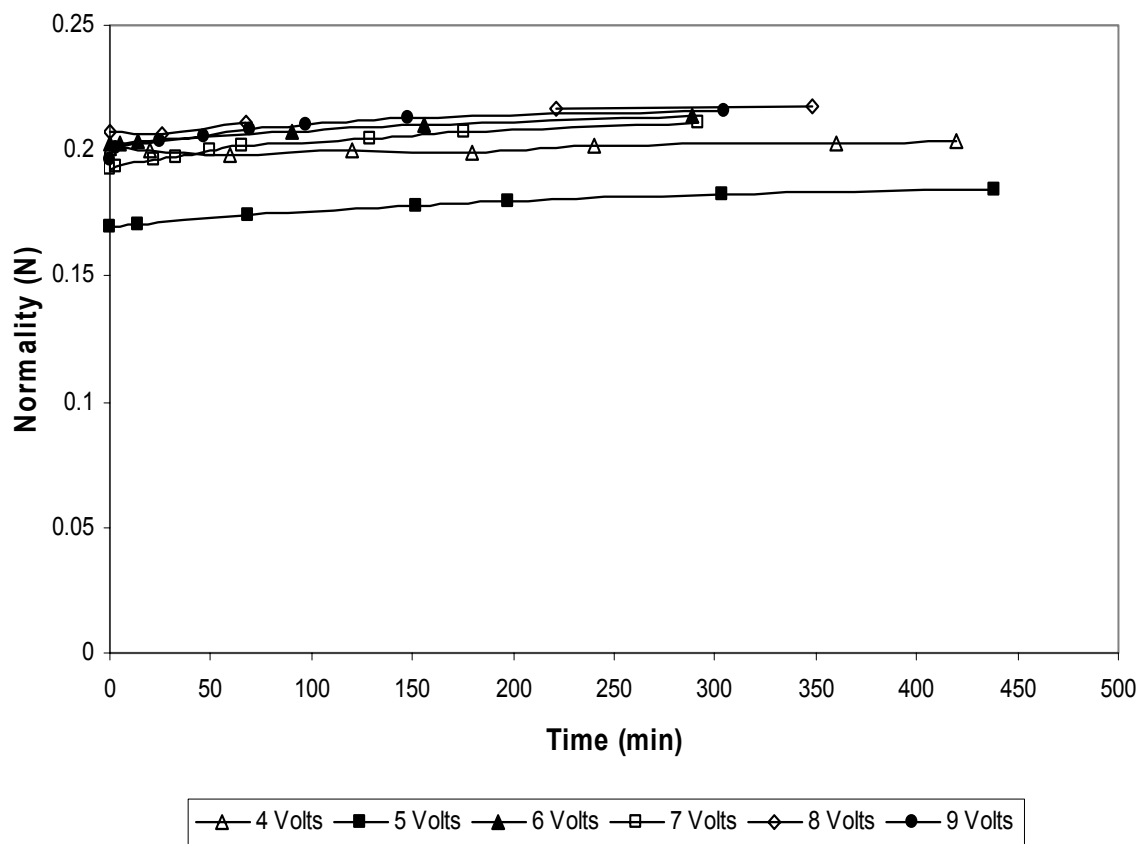


Figure 30. Normality of potassium hydroxide as a function of time at constant applied voltages.

Table 16. Normality of potassium hydroxide at constant applied voltage.

Voltages (Volts)	Initial Normality (N)	Final Normality (N)	Increase Percentage (%)
4	0.2007	0.2035	1.39
5	0.1700	0.1849	8.76
6	0.2029	0.2139	5.42
7	0.1930	0.2112	9.42
8	0.2073	0.2174	4.89
9	0.1961	0.2157	10.02

CHAPTER 5

CONCLUSIONS

Under batch recirculation operation mode at constant applied voltage, it was found that the current density, pH and electrical conductivity decreased as a function of the time, as result of ions removal and demineralization of wheat solution. The initial electrical resistance of electrolytic cell is constant as consequence of similar initial conditions of the solutions used in the experiments.

High nitrate and potassium removals were obtained at 5, 6, 7, 8 and 9 volts. Anions removals over 90% were obtained after 200 minutes of operation at these constant applied voltages. At 4 volts the ions removal is lower due to back diffusion resulting from effect of membrane fouling and a selectivity decrease because the active sites of anion membrane are taken by anion organic molecules. The maximum nitrate and potassium removal of 100 % and 99.82%, respectively, was obtained at 9 Volts. The results of anions removal as function of time shown that the anion membranes selectivity used in this study were more efficient in the removal of monovalent anions (NO_3^- and Cl^-) than for divalent anion and trivalent anion (SO_4^{2-} and PO_4^{3-} respectively). There isn't a significant difference between selectivity of monovalent and divalent cations of cation-exchange membrane.

At low voltages, the electrical resistance increase, as indicator of membrane fouling. This is possible due to higher due to low ions mobility through the anion membrane. The electrical resistance of the system, fluid and

anion membrane, increase with the time; at 100 mV, the electrical resistance increase is lower than at 75mV and 25 mV, maybe due to effects of the voltage over the wheat leachate solution. At 75 mV, the fluid electrical resistance increase is higher. The electrical resistance increase of fluid is due to decrease of conductivity and anion organic molecule concentration.

It is demonstrated that the wheat leachate solution has a high concentration of anion organic molecules. The experiments of electrical resistance with cation-exchange membrane yielded a poor decrease of electrical resistance of the system (wheat leachate solution and cation membrane), as consequence of a low concentration of cation organic molecules. It is possible that the wheat leachate solution contain cation organic molecules of high molecular weight and of low concentration. This would explain why there isn't fouling at low voltages and because the electrical resistance of cation membrane (or fouling membrane) increases with the time at high voltages.

BIBLIOGRAPHY

- Allison, R. P. Electrodialysis reversal in water reuse applications. *Desalination*. 103:11-18; 1995.
- Amor, Z.; Bariou, B.; Mameri, N.; Taky, M.; Nicolas, S., and Elmidaoui, A. Fluoride removal from brackish water by electrodialysis. *Desalination*. 133: 215-223; 2001
- Andres, L. J.; Riera, F. A.; and Alvarez, R. Recovery and concentration by electrodialysis of Tartaric acid from fruit juice industries waste waters. *J. Chem. Technol. Biotechnol.* 70:247-252; 1997.
- Cattoir, S.; Smets, D, and Rahier, A. The use of electro-electrodialysis for the removal of sulphuric acid from decontamination effluents. 121: 123-130; 1999.
- Chen, J. J. J.; Qian, K. X., and Zhao, J. C. Resistance due to the presence of bubbles in an electrolytic cell with a grooved anode. *Trans IChemE*, 79: Part A, 383-388; 2001.
- Cherif, A. T.; Molenat, J., and Elmidaoui, A. Nitric acid and sodium hydroxide generation by electrodialysis using bipolar membranes. *J. Applied Electrochemistry*. 27: 1069-1074; 1997.
- Colon, G., and Rosenau, J. R. Lactic acid recovery from fermented acid-cheese whey via electrodialysis, *AIChE Technical Paper*, AIChE Annual Meeting, New York, 1987.
- Colon G., and Sager, J. C. Electrolytic removal of nitrate from crop residues. *Life Support Biosphere Sci.* 7:301-310; 2001.
- Curet, M. Removal of nitrate and potassium from wheat leachate using a four compartment electrolytic cell. University of Puerto Rico. 2000
- Dorsheimer, W. T., C. B. Drewery, D. P. Fritsch and D. E. Williams. Removing nitrate from groundwater. *Water Engineering and Management*. 144(12): 20-24; Dec 1997.
- Elmidaoui, A.; Elhannouni, F. ; Menkouchi, M. A. ; Chay, L. ; Elabbassi, H. ; Hafsi, M. , and Largeteau, D. Pollution of nitrate in Moroccan ground water: removal by electrodialysis. 136: 325-332; 2001.

- Eyal, A., and Kendem, O. Nitrate-selective anion exchange membranes. *J. Membr. Sci.* 38: 101-111; 1988.
- Finger, B. W., and R. F. Strayer. Development of an intermediate scale aerobic bioreactor to regenerate nutrients from inedible crop residues SAE Tech. Pap. 941501. 1994
- Flett, D. S. Ion Exchange Membranes. Ellis Horwood: Chichester, 1983.
- Fonseca, A. D., J. G. Crespo, J. S. Almeida and M. A. Reis. Drinking water denitrification using a novel ion-exchange membrane bioreactor. *Environmental Science and Technology* 34(8): 677-684. 2000.
- Garland, J. L. and Mackowiack, C. M. Utilization of water soluble fraction of wheat straw as a plant nutrient source. NASA Tech. Memorandum 103497, 1990.
- Garland, J. L. Characterization of the water soluble components of inedible residues from candidate CELSS crop. NASA Tech. Memorandum 107577, 1992.
- Garland, J. L.; Mackowiack, C. M. and Sager, J. C. Hydroponic crop production using recycled nutrients from inedible crop residues. SAE Tech. Paper 932173; 1993
- Gordils, N. E., and Colón, G. Removal of sodium chloride from human urine via batch recirculation electrodialysis at constant applied voltage. *Habitation.* 9: 47-57; 2003.
- Grossman, G., and Sonin, A. Experimental study of the effects of hydrodynamics and membrane fouling in electrodialysis. *Desalination.* 10: 157-180; 1972.
- Hanley, T. R., and Chiu, H-K. Phosphoric acid concentration by electrodialysis. *AICHE Symposium Series. Industrial Membrane Processes.* 82: 121-132; 1986.
- Kesore, K.; Janowski, F., and Shaposhnik, V. A. Highly effective electrodialysis for selective elimination of nitrates from drinking water. *J. Membrane Science.* 127:17-24; 1997.
- Kim, Y. H., and Moon, S. H. Lactic acid recovery from fermentation broth using one stage electrodialysis. *J. Chem. Technol. Biotechnol.* 76:169-178; 2001.

- Korngold, E. Electrodialysis-membranes and mass transport. In: George, B., ed. Synthetic membrane processes. Fundamentals and water applications. New York: Academic Press; 1984:191-220; 1984.
- Lee, H.-J.; Choi, J.-H.; Cho J., and Moon, S.-H. Characterization of anion exchange membranes fouled with humate during electrodialysis. J. Membrane Science. 203: 115-126; 2002.
- Lindstrand, V.; Jönsson, A.-S, and Sundström, G. Organic fouling of electrodialysis membranes with and without applied voltage. Desalination. 130: 73-84; 2000.
- Lindstrand, V.; Jönsson, A.-S, and Sundström, G. Fouling of electrodialysis membranes by organic substances. Desalination. 128: 91-102; 2000.
- Mackie, G. L. 2001. Applied Aquatic Ecosystem Concepts. Iowa: Kendall/Hunt Publishing Company.
- Maurel, A. Dessalement des Eeaux Par Electrodialysis test bed plant. Techniques de l'ingenieur . C. E. N., Cadarach. 1972
- Moon, P. J.; Parulekar, S. J., and Tsai, S.-P. Competitive anion transport in desalting of mixtures of organic acids by batch electrodialysis. J. Membrane Science. 141:75-89; 1998.
- Saracco, G.; Zanetti, M. C., and Onofrio, M. Novel application of monovalent-ion-permselective membranes to the recovery treatment of an industrial wastewater by electrodialysis. 32: 657-662; 1993.
- Shah, P. M., and Scamehorn, J. F. Use of electrodialysis to deionize acidic wastewater streams. Ind. Eng. Chem. Res. 26:No.2, 269-277; 1987.
- Urano, K.; Ase, T., and Naito, Y. Recovery of acid from wastewater by electrodialysis. Desalination. 51: 213-226; 1984.